THE JOURNAL OF BIOLOGICAL CHEMISTRY VOL. 291, NO. 36, pp. 18880–18896, September 2, 2016

Activation of the Yeast *UBI4* Polyubiquitin Gene by Zap1 Transcription Factor via an Intragenic Promoter Is Critical for Zinc-deficient Growth*

Received for publication, June 10, 2016, and in revised form, July 8, 2016 Published, JBC Papers in Press, July 18, 2016, DOI 10.1074/jbc.M116.743120

Colin W. MacDiarmid[‡], Janet Taggart[‡], Jeeyon Jeong[§], Kittikhun Kerdsomboon[‡], and David J. Eide[‡1]

From the [‡]Department of Nutritional Sciences, University of Wisconsin, Madison, Wisconsin 53706 and [§]Department of Biology, Amherst College, Amherst, Massachusetts 01002

Stability of many proteins requires zinc. Zinc deficiency disrupts their folding, and the ubiquitin-proteasome system may help manage this stress. In *Saccharomyces cerevisiae*, *UBI4* encodes five tandem ubiquitin monomers and is essential for growth in zinc-deficient conditions. Although *UBI4* is only one of four ubiquitin-encoding genes in the genome, a dramatic decrease in ubiquitin was observed in zinc-deficient *ubi4*Δ cells. The three other ubiquitin genes were strongly repressed under these conditions, contributing to the decline in ubiquitin. In a screen for *ubi4*Δ suppressors, a hypomorphic allele of the *RPT2* proteasome regulatory subunit gene (*rpt2*^{E301K}) suppressed the *ubi4*Δ growth defect. The *rpt2*^{E301K} mutation also increased ubiquitin accumulation in zinc-deficient cells, and by using a ubiquitin-independent proteasome substrate we found that proteasome activity was reduced. These results suggested that increased ubiquitin supply in suppressed *ubi4*Δ cells was a consequence of more efficient ubiquitin release and recycling during proteasome degradation. Degradation of a ubiquitin-dependent substrate was restored by the *rpt2*^{E301K} mutation, indicating that ubiquitination is rate-limiting in this process. The *UBI4* gene was induced ~5-fold in low zinc and is regulated by the zinc-responsive Zap1 transcription factor. Surprisingly, Zap1 controls *UBI4* by inducing transcription from an intragenic promoter, and the resulting truncated mRNA encodes only two of the five ubiquitin repeats. Expression of a short transcript alone complemented the *ubi4*Δ mutation, indicating that it is efficiently translated. Loss of Zap1-dependent *UBI4* expression caused a growth defect in zinc-deficient conditions. Thus, the intragenic *UBI4* promoter is critical to preventing ubiquitin deficiency in zinc-deficient cells.

Zinc is an essential element with diverse roles in biology. Unlike transition metals, such as iron and copper, zinc ions (Zn^{2+}) are not redox-active under physiological conditions and do not play a direct role in redox reactions. Zn^{2+} strongly interacts with ligands, such as cysteine, histidine, and acidic amino acids in proteins (1). When bound by three or fewer ligands, Zn^{2+} can act as a Lewis acid to facilitate catalysis by diverse classes of enzymes, including oxidoreductases, transferases, and hydrolases (2). In contrast, binding of Zn^{2+} by four ligands produces a relatively inert, structurally rigid tetrahedral complex, which provides stability to many classes of protein domains (1–3). Because of its catalytic and structural roles, Zn^{2+} has been estimated to be required for the folding and function of ~10% of proteins encoded by eukaryotic genomes and ~5% of proteins in prokaryotes (4, 5). One abundant example is the enzyme alcohol dehydrogenase, which contains two Zn^{2+} atoms per subunit, one serving in catalysis and the other playing a structural role (1, 6, 7). Consistent with the importance of zinc to Adh[2] folding, mutants of Adh lacking structural zinc site ligands are unstable and quickly degraded *in vivo* (8).

Although zinc is essential, it is also toxic in excess, and organisms have evolved mechanisms to regulate zinc accumulation in response to changes in external supply and intracellular stores. In the yeast *Saccharomyces cerevisiae*, the Zap1 transcriptional activator regulates ~80 genes in response to zinc status (9–11). Zap1 binds to a conserved sequence, the zinc-response element (ZRE) (5′-ACCTTNAAGGT-3′), found in one or more copies in the promoters of its target genes (12). Zap1 itself contains seven zinc finger motifs, five of which play structural roles in the DNA-binding domain. The remaining two fingers are contained in an activation domain (AD2) and serve a regulatory function. The AD2 zinc fingers are variants of the classic C_2H_2 zinc finger with higher Zn^{2+} lability. Binding of Zn^{2+} to these domains represses Zap1 activation domain function and the transcription of its target genes (13). Zinc status also regulates the activity of a second activation domain (AD1) (14) and controls the activity of the DNA-binding domain independently of AD function (15).

Analysis of the Zap1 regulon revealed that zinc-regulated genes can be sorted into two basic classes: "homeostatic" genes induced to maintain intracellular zinc supply and "adaptive" genes that may aid the survival of deficient cells without altering zinc status (11). Homeostatic genes include those required for zinc uptake across the plasma membrane (*ZRT1*, *ZRT2*, and

* This work was supported by National Institutes of Health Grant GM056285. The authors declare that they have no conflicts of interest with the contents of this article. The content is solely the responsibility of the authors and does not necessarily represent the official views of the National Institutes of Health.

[1] To whom correspondence should be addressed: Dept. of Nutritional Sciences, 1415 Linden Dr., University of Wisconsin-Madison, Madison, WI 53706-1571. Tel.: 608-263-1613; Fax: 608-262-5860; E-mail: eide@nutrisci.wisc.edu.

[2] The abbreviations used are: Adh, alcohol dehydrogenase; ZRE, zinc-response element; AD, activation domain; LZM, low zinc medium; YPD, yeast extract-peptone-dextrose; Ub, ubiquitin; RP, ribosomal subunit protein; RT-qPCR, quantitative RT-PCR; mODC, mouse ornithine decarboxylase; VHL, von Hippel-Lindau; HSE, heat shock element; RLM, RNA ligase-mediated; RACE, rapid amplification of cDNA ends; SD, synthetic defined.

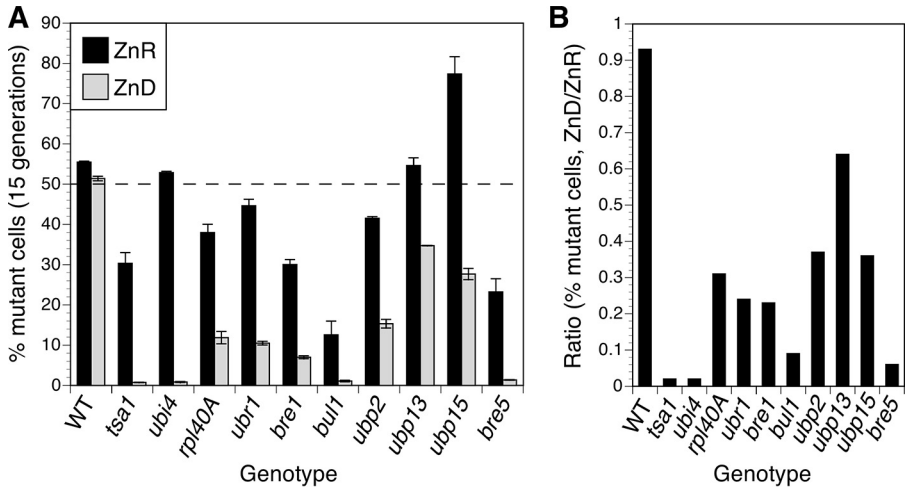

FIGURE 1. **Many mutants defective for ubiquitin metabolism show growth defects in low zinc.** *A*, analysis of growth by flow cytometry. Untagged wild-type (BY4743) cells or isogenic mutants of the indicated genotype were mixed with approximately equal numbers of GFP-expressing BY4743 cells, inoculated into zinc-replete (*ZnR*; LZM + 100 μM $ZnCl_2$) or zinc-deficient (*ZnD*; LZM + 1 μM $ZnCl_2$) medium, and grown for 15 generations prior to analysis. Approximately 20,000 total cells per culture were assessed for GFP fluorescence by flow cytometry, and the graph shows the percentage of untagged cells in the cultures. The data are the means from six replicate cultures, and the error bars indicate ±1 S.D. The *dashed line* at 50% indicates the expected result if both mutant and wild-type cells grew equally well. *B*, the mean percentages of untagged (control or mutant) cells in the zinc-deficient cultures divided by their percentages in the zinc-replete cultures. Ratios less than 1.0 indicate a stronger growth defect in zinc-deficient medium.

FET4) and for redistribution of zinc between the cytosol and intracellular compartments (*ZRT3*, *ZRG17*, and *ZRC1*). Adaptive zinc-regulated genes include those involved in fermentation (*ADH1* and *ADH4*) (16), phospholipid synthesis (*PIS1*, *CKI1*, and *EKI1*) (17, 18), sulfur metabolism (*MET30*) (19), resistance to oxidative stress (*CTT1*), and NADPH production (*TKL2*).

One intriguing member of the adaptive class of Zap1 target genes is *TSA1*, which encodes a dual function thioredoxin-dependent peroxidase and protein chaperone. Tsa1 function is essential for growth of zinc-deficient cells (20). Our initial studies indicated a role of the Tsa1 peroxidase activity in protecting zinc-deficient cells against an elevated level of reactive oxygen species in zinc-deficient cells. More recently, we found that the Tsa1 protein chaperone activity was more important than the peroxidase function for growth in zinc-deficient conditions (21). Zinc-deficient cells lacking Tsa1 chaperone activity accumulated elevated levels of stress-responsive protein chaperones, suggesting elevated unfolded protein accumulation and a corresponding heat shock response. Also consistent with this hypothesis, zinc-deficient *tsa1*Δ cells accumulated distinct cytoplasmic foci marked by the Hsp104 disaggregase chaperone. These foci resembled the insoluble protein deposit (or "IPOD"), a compartment that accumulates in cells blocked from degrading model misfolded proteins (22). Our observations suggested that zinc-deficient cells accumulate aggregates of unfolded proteins because they lack the needed supply of Zn^{2+} cofactor for binding to structural zinc sites. Under these conditions, the Tsa1 chaperone may stabilize zinc-dependent apoproteins and shield them from misfolding and aggregation or maintain them in a state competent for efficient degradation.

Other evidence also links the protein homeostasis machinery with survival of low zinc stress. Several candidate Zap1 target genes encode proteins with roles in protein homeostasis, including a molecular chaperone (*HSP26*), and proteins involved in autophagy (*ATG19*, *ATG41*, and *UTH1*) and vacuolar proteolysis (*PRB1*, *PRC1*, and *PEP4*) (11). By functional genomics analysis, we also identified genes that were important for survival in low zinc but were not known Zap1 targets (23). These genes encode another protein chaperone (*HSP42*) as well as factors important for autophagy (*ATG3*, *ATG8*, and *ATG15*). Of particular interest was the identification of a number of genes encoding components of the ubiquitin system, including the major source of stress-induced ubiquitin, *UBI4*. Protein degradation via the ubiquitin-proteasome system is one potential mechanism for the elimination of aggregated or misfolded proteins from zinc-deficient cells, and the loss of this system might aggravate unfolded protein stress caused by zinc deficiency. To explore this hypothesis, we investigated the role of *UBI4* in tolerance to zinc deficiency.

Results

Ubiquitin Metabolism Genes Are Required for Optimal Growth under Zinc-deficient Conditions—Our previous functional genomics screen identified many gene deletion mutations that caused slower cell growth in a zinc-limiting medium (23). These included several genes involved in ubiquitin metabolism, such as those encoding ubiquitin itself (*UBI4* and *RPL40A*), E3 ubiquitin ligase components (*UBR1*, *BRE1*, and *BUL1*), and ubiquitin-specific proteases (*UBP2*, *UBP13*, *UBP15*, and *BRE5*). To confirm the results of this genome-wide analysis and compare the relative effect of the mutations in more detail, we tested growth of the individual mutants. In pairwise competitive growth assays, wild-type cells expressing GFP were mixed with approximately equal numbers of untagged mutant cells and inoculated at low density into zinc-replete (low zinc medium (LZM) + 100 μM $ZnCl_2$) or zinc-limiting (LZM + 1 μM $ZnCl_2$) growth medium. The mixed cultures were then grown for 15 generations, and ~20,000 cells per culture were assessed as GFP-positive (wild-type) or GFP-negative (mutant) cells by flow cytometry (Fig. 1*A*). As expected, when the GFP-tagged wild-type strain was co-cultured with an untagged wild-type strain, the strains showed similar relative

growth in zinc-replete and -limiting conditions. A *tsa1*Δ mutant included as a positive control showed a severe growth defect relative to wild type in zinc-deficient conditions with the final culture containing less than 1% mutant cells. Zinc-replete cultures also contained fewer *tsa1*Δ mutant cells (~30% of the total), indicating that this mutant has a milder but still detectable growth defect in replete conditions. Similarly, several of the ubiquitin-related mutants showed a growth defect in replete conditions, but in each case the defect in zinc-deficient conditions was more severe. Mutants disrupted for *UBP15* were surprising because they significantly outgrew wild-type cells in replete zinc conditions; the reason for this growth advantage is unclear.

To focus on how zinc status affected growth of these mutants, we calculated a ratio representing the severity of the zinc-deficient defect relative to zinc-replete growth (Fig. 1*B*). This ratio demonstrates that all of the mutant strains had a more severe growth defect in deficient conditions. These data confirmed that several genes related to ubiquitin production, recycling, and utilization are required for optimal zinc-limited growth. Notably, a *ubi4*Δ mutant showed no defect in zinc-replete medium but grew very poorly in low zinc. The severity of this phenotype and the central importance of ubiquitin for protein homeostasis led us to further investigate *UBI4*.

*The ubi4*Δ *Mutant Has an Increased Requirement for Zinc*—To further characterize the *ubi4*Δ mutant growth phenotype, we compared growth of wild-type and *ubi4*Δ cells over time in zinc-replete (Fig. 2*A*) or zinc-deficient medium (Fig. 2*B*). Consistent with the competitive growth assay, *ubi4*Δ cells grew as well as the wild-type strain in zinc-replete medium, but in deficient conditions *ubi4*Δ mutants showed an almost immediate slowing of growth after transfer to low zinc. To identify the level of zinc required to restore normal growth of *ubi4*Δ cells, wild-type and mutant cells were grown in the zinc-limiting medium supplemented with a range of zinc concentrations (Fig. 2*C*). Growth of *ubi4*Δ cells was significantly impaired relative to wild-type cells in media containing 1–2 μM zinc, but this effect was eliminated with 3 μM or higher added zinc. These results indicate that *UBI4* is only required under severely zinc-deficient conditions.

The effect of the *ubi4*Δ mutation on growth yield could be due to slowed or arrested growth, or it could reflect a loss of viability. We examined the effect of zinc deficiency on *ubi4*Δ cell viability as defined by the ability to form colonies on a zinc-replete medium after growth in zinc-deficient conditions. In comparison with a wild-type strain for which viability remained high, viability of *ubi4*Δ cells dropped rapidly after inoculation into low zinc, reaching ~10% of initial viability by 18 h (Fig. 2*D*). Thus, *ubi4*Δ mutants rapidly lose viability during low zinc stress.

The low zinc medium used in these experiments is specifically zinc-limiting for growth but also contains low available levels of other metal nutrients, such as iron, copper, and manganese. To test whether the growth defect of *ubi4*Δ was specific to zinc deficiency and not deficiency of other metals, we examined growth of *ubi4*Δ in zinc-limited medium supplemented with zinc or other metals. Although adding 100 μM zinc restored *ubi4*Δ growth to wild-type levels, supplementing 100 μM iron, copper, manganese, or cobalt had no effect (Fig. 2*E*). As a complementary approach, we made rich YPD medium copper- or iron-limiting by adding the copper chelator bathocuproine disulfonate or the iron chelator bathophenanthroline disulfonate, respectively. Adding either chelator slowed growth, and growth was restored by adding back the cognate metal, but *ubi4*Δ mutants were not more sensitive to either copper or iron chelation (Fig. 2*F*). These results indicate that the growth defect of *ubi4*Δ mutants is specific to zinc deficiency.

UBI4 Is the Primary Source of Ubiquitin in Zinc-limited Cells—To investigate the role of *UBI4* in zinc-deficient cells, we examined the effect of zinc status and *ubi4*Δ mutation on ubiquitin accumulation. *UBI4* encodes a translational fusion of five tandem ubiquitin monomers. Three other genes in yeast, *RPL40A* (*UBI1*), *RPL40B* (*UBI2*), and *RPS31* (*UBI3*), encode ubiquitin as fusions to ribosomal subunit proteins (Ub-RP). Once produced, these four fusion proteins are cleaved to release monomeric ubiquitin. Adequate ubiquitin supply is essential for growth, suggesting that *UBI4* is the primary source of ubiquitin for zinc-deficient cells. To test this prediction, we measured the level of protein-ubiquitin conjugates and free ubiquitin monomer accumulated by wild-type and *ubi4*Δ cells in zinc-replete and -deficient conditions (Fig. 3*A*). In wild-type cells, zinc deficiency increased ubiquitin conjugate accumulation ~2-fold relative to zinc-replete cells but reduced ubiquitin monomer accumulation by approximately the same degree. In the *ubi4*Δ mutant, zinc deficiency reduced the level of ubiquitin conjugate accumulation almost 70%, whereas ubiquitin monomers were undetectable. These results argue that *UBI4* is the dominant source of ubiquitin in cells under zinc-deficient conditions and that the *ubi4*Δ growth defect is a consequence of inadequate ubiquitin supply.

The reduced level of ubiquitin in zinc-deficient *ubi4*Δ cells could also be influenced by decreased expression of the other ubiquitin-encoding genes. To address this question, we measured the expression of the four ubiquitin genes in wild-type and *ubi4*Δ cells under zinc-replete and -deficient conditions using quantitative RT-PCR (RT-qPCR). In wild-type cells, zinc-deficiency reduced the expression of *RPL40A*, *RPL40B*, and *RPS31* to about 30% of the level seen in replete cells (Fig. 3*B*). Although the *ubi4*Δ mutation had little effect on the expression of these genes in replete cells, it caused a substantial additional decrease in their expression in low zinc. These observations suggested that the low level of ubiquitin observed in deficient *ubi4*Δ cells was due to the loss of *UBI4* contribution as well as further diminished expression of the other ubiquitin genes.

Ribosomal subunit genes are coordinately regulated with cell growth rate and repressed by stress conditions that slow growth, such as zinc deficiency. To assess whether the effects of zinc status and *ubi4*Δ mutation on Ub-RP gene expression were linked to regulation of ribosome biogenesis, we examined expression of *RPL1B*, which encodes the ribosomal 60S subunit protein L1B. The expression profile of *RPL1B* was very similar to the Ub-RP fusion genes, suggesting that their decreased expression is due to growth-responsive regulation of ribosome biogenesis (Fig. 3*B*). In contrast to these genes, *UBI4* expression in wild-type cells was induced ~5-fold in zinc-deficient cells.

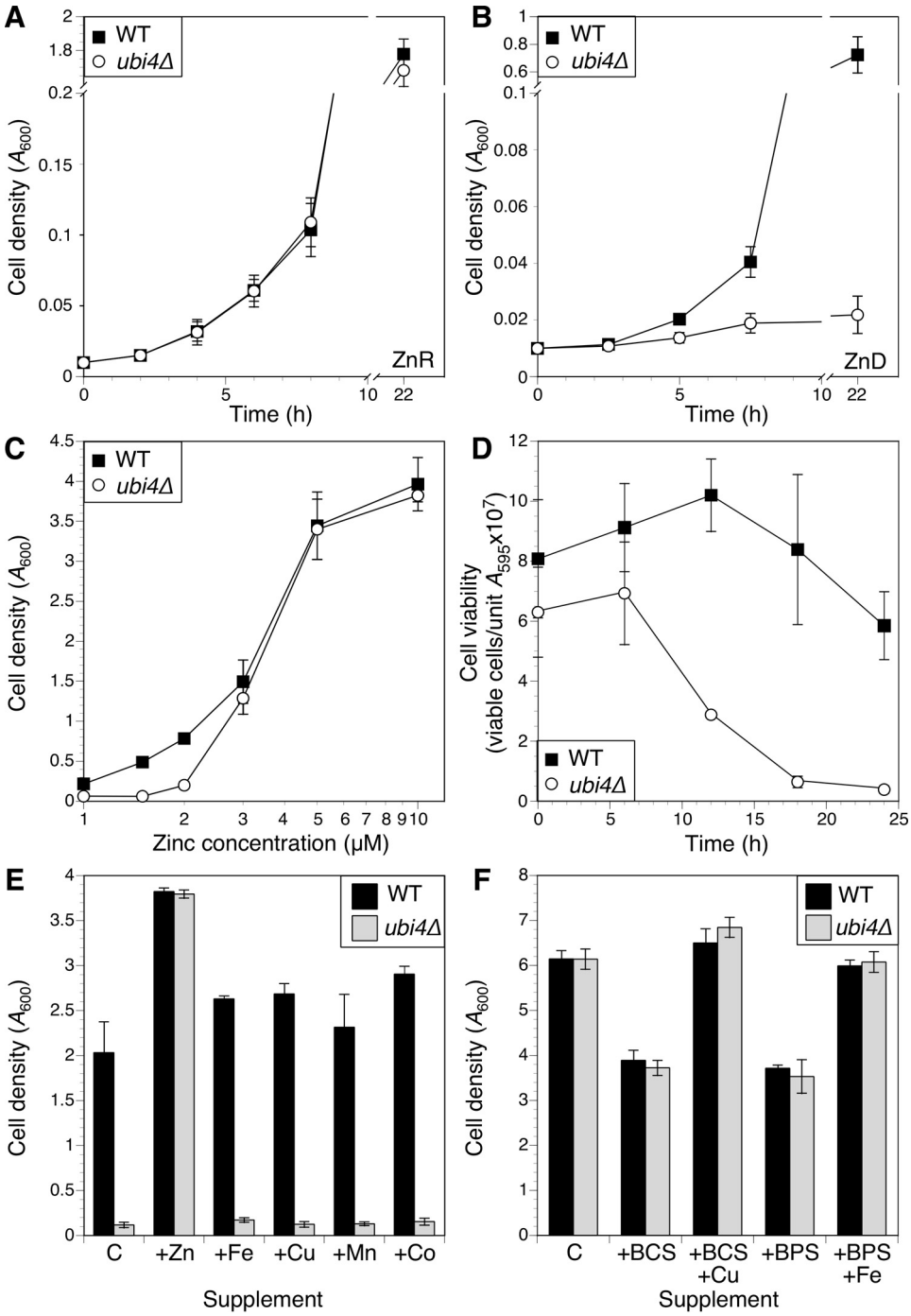

FIGURE 2. ***ubi4*Δ mutants exhibit a severe growth defect in zinc-deficient conditions.** *A* and *B*, time course of wild-type (BY4741) and isogenic *ubi4*::*KanMX4* mutant growth in zinc-replete (*ZnR*; *A*) or zinc-deficient (*ZnD*; *B*) medium (LZM with 100 or 1 μM added zinc, respectively). Cultures were inoculated with log phase cells to a starting A_{600} of 0.01, and culture densities were recorded at the indicated times. *C*, effect of varying zinc concentration on growth of wild-type and *ubi4*Δ strains. Cultures were inoculated as described for *A*, and cell densities were measured after 48-h incubation. *D*, log phase cultures of wild-type and *ubi4*Δ mutant cells in zinc-replete medium were used to inoculate zinc-deficient medium. Cell viability was monitored over time by plating aliquots on YPD plates and counting colony-forming units following 2 days of incubation. *E*, the *ubi4*Δ growth defect in zinc-deficient medium is rescued specifically by zinc. Aliquots of LZM + 1 μM added zinc were supplemented with 100 μM $ZnCl_2$, $FeCl_3$, $CuCl_2$, $MnCl_2$, or $CoCl_2$ and inoculated with wild-type or *ubi4*Δ cells as described for *A*. Control (*C*) indicates LZM + 1 μM $ZnCl_2$ with no additional metal supplement. Cell densities were measured after 48 h. *F*, a *ubi4*Δ mutant was not hypersensitive to copper or iron deficiency. Aliquots of YPD were supplemented with 100 μM copper chelator bathocuproine disulfonic acid (*BCS*) or iron chelator bathophenanthroline disulfonate (*BPS*) with or without 100 μM added $CuCl_2$ or $FeCl_3$ and inoculated with wild-type or *ubi4*Δ cells as described for *A*. Control (*C*) indicates YPD with no additional metal or chelator supplement. Cultures were grown for 24 h, and cell densities were recorded. For all panels, data points represent averages of three independent cultures, and *error bars* denote ±1 S.D.

These data are consistent with the induction of *UBI4* being required to compensate for the decreased expression of Ub-RP fusion genes in zinc-deprived cells.

*Reduction of Proteasome Activity Suppresses the ubi4*Δ *Mutation*—Ubiquitin plays a variety of roles in cells. To probe the role of *UBI4* and ubiquitin in zinc-deficient cells, we

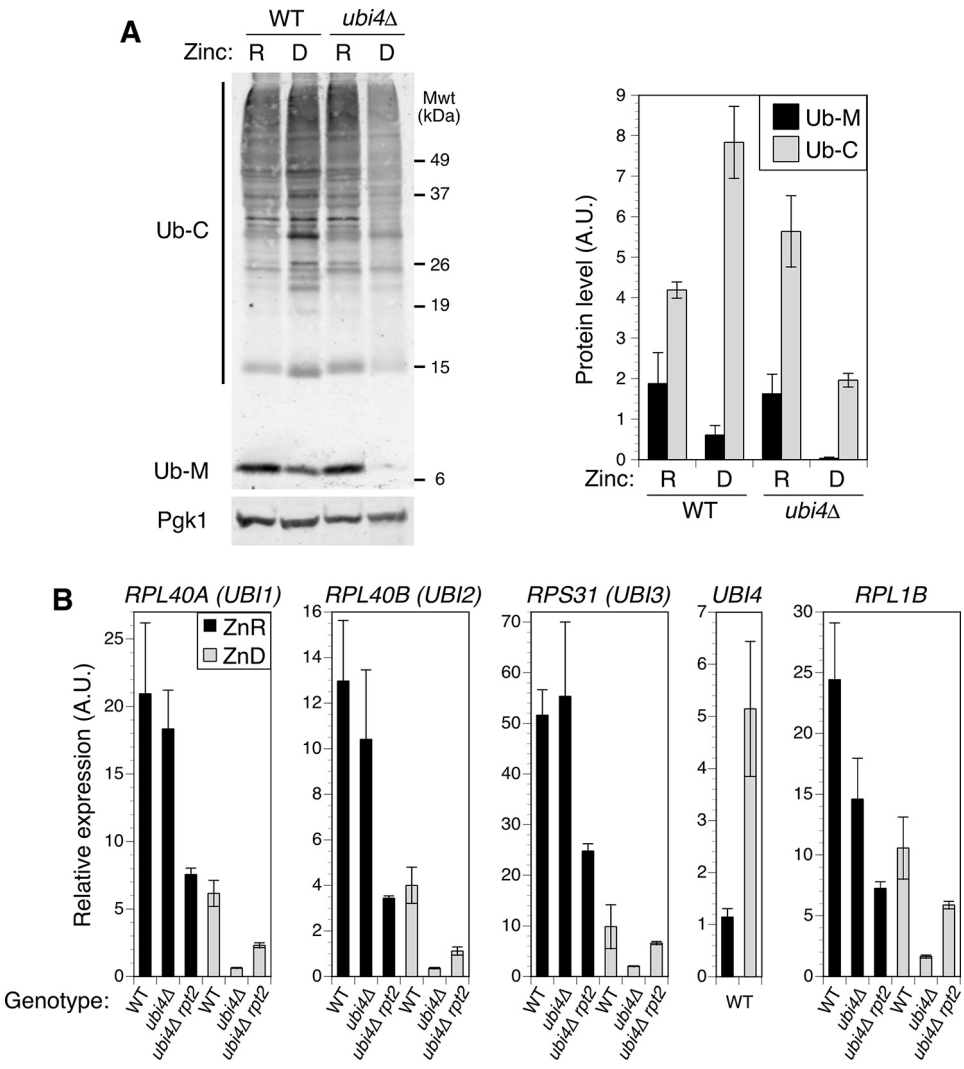

FIGURE 3. **UBI4 is the predominant source of ubiquitin for zinc-limited cells.** *A*, wild-type (BY4741) and *ubi4*::*KanMX4* cells were grown in zinc-deficient (*D*; LZM + 1 μM $ZnCl_2$) or zinc-replete (*R*; LZM + 100 μM $ZnCl_2$) medium. The abundance of ubiquitin and a loading control protein (Pgk1) was assayed by immunoblotting (one representative immunoblot is shown). Levels of ubiquitin conjugates (*Ub-C*) and monomeric ubiquitin (*Ub-M*) were quantified from three replicates. *B*, effect of zinc status and *ubi4*Δ mutation on expression of ubiquitin precursor genes and the ribosomal subunit gene *RPL1B*. Wild-type (BY4741), *ubi4*::*KanMX4*, and *ubi4*Δ *rpt2*^{E301K} (CWM280) cells were grown to log phase in SD medium and then used to inoculate zinc-deficient (*ZnD*; LZM + 1 μM $ZnCl_2$) or -replete (*ZnR*; LZM + 100 μM $ZnCl_2$) medium at low starting densities. Cultures were maintained in log phase by dilution with fresh media for 24 h. The mRNA abundance of the indicated genes was then determined by RT-qPCR. Target transcript abundance was normalized to the average abundance of three control transcripts (18S rRNA, *TAF10*, and *ACT1*). All plotted data points represent the means of three replicates, and *error bars* denote ±1 S.D. *A.U.*, arbitrary units.

screened for suppressor mutations that restored zinc-limited growth to *ubi4*Δ cells. A pool of mutagenized *ubi4*Δ cells was used to inoculate multiple independent cultures of zinc-limiting medium, and suppressed clones were isolated from cultures that reached high density. One suppressor mutation was identified from a selected recessive suppressor mutant via pooled linkage analysis with whole genome sequencing (24). The suppression phenotype was linked to a missense mutation in the *RPT2* gene that substituted lysine for glutamate at amino acid 301 (E301K). This mutation restored an almost wild-type rate of growth to the *ubi4*Δ mutant in zinc-limited conditions (Fig. 4*A*). *RPT2* is an essential gene encoding one of the ATPase subunits of the regulatory particle of the 26S proteasome (25). The recessive, non-lethal nature of the *rpt2*^{E301K} mutation suggested that it was a hypomorphic allele. To confirm that the *rpt2*^{E301K} mutation was responsible for *ubi4*Δ suppression, we cloned the wild-type *RPT2* gene and demonstrated that it complemented the suppression phenotype (data not shown).

The regulatory particle ATPase subunits act in substrate transfer to the proteasome core particle for degradation. Although ubiquitin is usually released and recycled prior to substrate degradation, a significant fraction of it is degraded by the proteasome along with the substrate under stress conditions (26). Therefore, we reasoned that the *rpt2*^{E301K} mutation might slow the rate of substrate protein transfer to the core particle, thereby increasing the likelihood that the attached ubiquitin is released by proteasome-associated deubiquitinases and thus protected from degradation. Such a mechanism would increase ubiquitin levels in a suppressed *ubi4*Δ strain. To test this hypothesis, we examined the effect of *rpt2*^{E301K} on the level of ubiquitin conjugates and free monomers accumulated by *ubi4*Δ mutants. Immunoblots showed that the reduced accu-

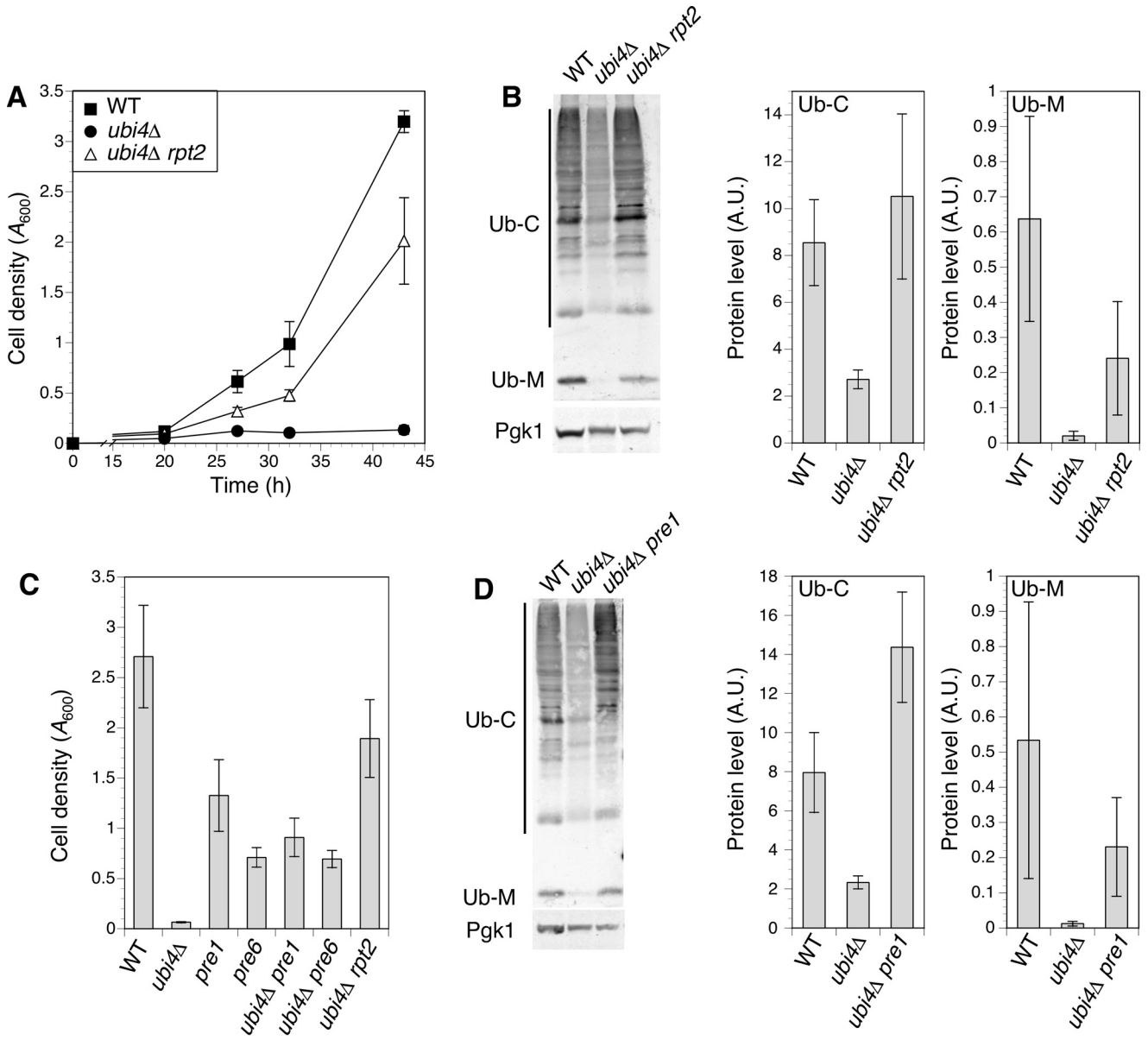

FIGURE 4. **Mutation of proteasome subunit genes restored ubiquitin supply and growth in zinc-deficient *ubi4*Δ cells.** *A*, a recessive *rpt2* allele suppressed the *ubi4*Δ growth defect in zinc-deficient conditions. Wild-type (BY4741), *ubi4*::*KanMX4*, and *ubi4*Δ *rpt2*^{E301K} (CWM280) strains were grown to saturation in SD medium and inoculated into zinc-deficient (LZM + 1 μM $ZnCl_2$) cultures. Growth was monitored by measuring cell densities. Each data point represents the mean of three independent cultures, and *error bars* show ±1 S.D. *B*, effect of the *rpt2*^{E301K} suppressor mutation on ubiquitin accumulation. Strains listed in *A* were grown in zinc-deficient conditions and assayed for ubiquitin by immunoblotting. One representative immunoblot is shown. Pgk1 was detected as a loading control. Adjacent panels show quantitation of ubiquitin conjugates (*Ub-C*) and monomers (*Ub-M*) in three replicate immunoblots including the example shown. *C*, hypomorphic alleles of the *PRE1* and *PRE6* proteasomal subunit genes suppressed the *ubi4*Δ growth defect in zinc-deficient conditions. Cell densities of wild-type (BY4741), *ubi4*Δ (CWM260), *pre1*^{DAmP}, *pre6* ^{DAmP}, *ubi4*Δ *rpt2*^{E301K} (CWM280), *ubi4*Δ *pre1* ^{DAmP} (CWM278), and *ubi4*Δ *pre6* ^{DAmP} (CWM279) strains were compared after 48 h of growth in zinc-deficient (LZM + 1 μM $ZnCl_2$) medium as described for *A*. Means of three replicates are shown; *error bars* represent ± 1 S.D. *D*, wild-type (BY4741), *ubi4*Δ (CWM260), and *ubi4*Δ *pre1*^{DAmP} (CWM278) cells were grown in zinc-deficient conditions and assayed for ubiquitin by immunoblotting. One representative immunoblot is shown, and Pgk1 was detected as a loading control. Adjacent panels show quantitation of ubiquitin conjugates (*Ub-C*) and monomers (*Ub-M*) in three replicate immunoblots including the example shown. *A.U.*, arbitrary units.

mulation of both conjugates and monomers in zinc-deficient *ubi4*Δ cells was effectively reversed by the *rpt2*^{E301K} mutation (Fig. 4*B*).

If the *rpt2*^{E301K} mutation increased ubiquitin supply by decreasing the rate at which proteasome substrates were degraded, we predicted that inhibiting the activity of the core particle itself might also elevate ubiquitin supply and suppress the *ubi4*Δ growth defect. To test this prediction, we combined *pre1*^{DAmP} and *pre6*^{DAmP} hypomorphic alleles with *ubi4*Δ. *PRE1* encodes the β4 subunit of the core particle, and *PRE6* encodes the α4 subunit (27), and hypomorphic alleles of these genes would be expected to reduce the rate of proteasomal protein degradation. Although the *pre1*^{DAmP} *and pre6*^{DAmP} mutations alone caused a growth defect in zinc-deficient conditions relative to wild-type cells, they both effectively suppressed the growth defect caused by the *ubi4*Δ mutation (Fig. 4*C*). We also examined the effect of the *pre1*^{DAmP} mutation on ubiquitin levels in *ubi4*Δ cells and observed an increase in both ubiquitin

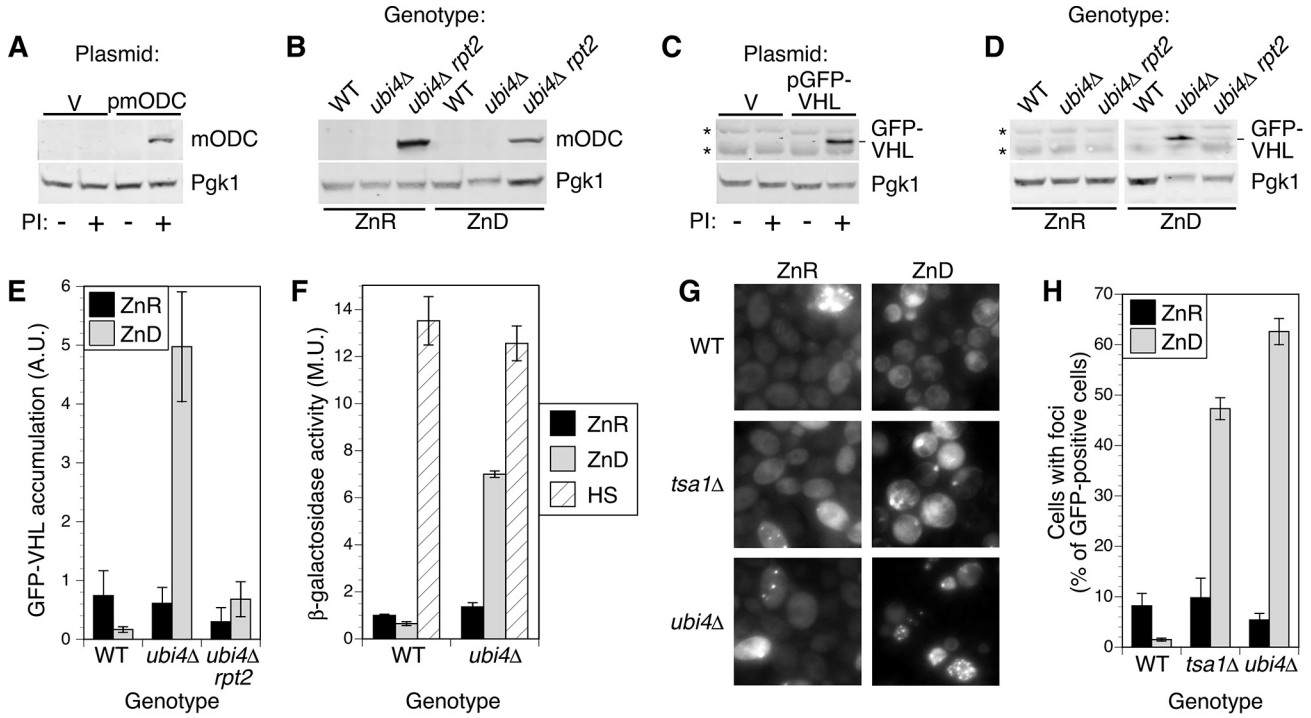

FIGURE 5. **Reduced proteasome activity restores ubiquitin-dependent degradation.** *A*, mODC accumulates following proteasome inhibition (*PI*). BY4743 *pdr5*Δ cells transformed with empty vector (pRS315; *V*) or p415-GFP-FLAG-mODC (*pmODC*; expressing FLAG-tagged mouse ornithine decarboxylase) were grown to log phase in LZM + 100 μM $ZnCl_2$ and treated for 1 h with DMSO carrier (−) or proteasome inhibitors (50 μM MG132 and 250 μM bortezomib; +) before harvesting. Protein extracts were analyzed by immunoblotting with anti-FLAG antibodies. *B*, mODC accumulates in *rpt2*^{E301K} mutants independently of zinc supply. Wild-type (BY4741), *ubi4*::*KanMX4*, and *ubi4*Δ *rpt2*^{E301K} (CWM280) strains transformed with p415-GFP-FLAG-mODC were grown to log phase in LZM + 100 μM $ZnCl_2$ (*ZnR*) or 1 μM $ZnCl_2$ (*ZnD*) prior to immunoblotting. *C*, GFP-VHL accumulates following proteasome inhibition. BY4743 *pdr5*Δ was transformed with empty vector (*V*) or pESC-LEU-GAL1p-GFP-VHL (*pGFP-VHL*; expressing GFP-tagged von Hippel-Lindau protein), and cells were assayed for mODC as described in *A*. The position of the GFP-VHL band is shown, and two nonspecific bands are indicated by *asterisks*. *D*, GFP-VHL is stabilized in zinc-deficient *ubi4*Δ cells and degraded in *ubi4*Δ *rpt2*^{E301K}. GFP-VHL accumulation was assayed as described for mODC in *B*. For all immunoblots in *A*–*D*, one blot representative of three replicates is shown, and Pgk1 was detected as a loading control. *E*, quantitation of GFP-VHL bands for three replicates, including the blot shown in *D*. *Error bars* denote ±1 S.D. *F*, expression of an Hsf1-regulated reporter gene in wild-type and *ubi4*Δ cells. Strains transformed with the pHSE-lacZ plasmid were grown to log phase in zinc-replete (*ZnR*; LZM + 100 μM $ZnCl_2$) or zinc-deficient (*ZnD*; LZM + 1 μM $ZnCl_2$) medium and assayed for β-galactosidase activity. As a positive control for reporter activity, aliquots of zinc-replete cells were also subjected to heat shock at 37 °C for 1 h before assay (*HS*). *G* and *H*, wild-type (BY4743), *tsa1*Δ, and *ubi4*Δ diploid strains transformed with pHSP104-GFP were grown in LZM + 1000 μM $ZnCl_2$ (*ZnR*) or 1 μM $ZnCl_2$ (*ZnD*) medium for at least four generations, maintaining cell density below an A_{595} of 0.4 by dilution with fresh media. Cells were examined by fluorescence microscopy to determine the proportion of cells with detectable GFP fluorescence that also displayed foci. Data points indicate the average of three replicates, and *error bars* show ±1 S.D. *A.U.*, arbitrary units; *M.U.*, Miller units.

conjugate and monomer accumulation (Fig. 4*D*). These observations indicate that a reduction in proteasome activity can increase ubiquitin supply and suppress the *ubi4*Δ low zinc growth defect.

To test whether the *rpt2*^{E301K} mutation did in fact reduce proteasome activity as hypothesized, we determined the effect of this mutation on the accumulation of a model proteasome substrate, mouse ornithine decarboxylase (mODC). mODC does not require ubiquitination to be degraded by the proteasome (28). Accumulation of mODC thus provides a measure of proteasome activity that is independent of ubiquitin availability, and its stability should be unaffected by the *ubi4*Δ mutation in zinc-deficient cells. As expected, mODC was not detected in zinc-replete wild-type cells but did accumulate in cells treated with proteasome inhibitors (Fig. 5*A*). Regardless of zinc supply, no mODC was detected in wild-type or *ubi4*Δ cells, indicating that intrinsic proteasome activity was not greatly diminished by zinc deficiency (Fig. 5*B*). In contrast, mODC was readily detected in both zinc-replete and -deficient *ubi4*Δ *rpt2*^{E301K} cells, confirming that the *rpt2*^{E301K} mutation constitutively inhibits proteasome activity.

Suppression of the *ubi4*Δ growth defect in low zinc by mutations that decrease proteasome function suggested the intriguing possibility that the ubiquitin-requiring processes critical for growth of these cells were unrelated to proteasomal degradation of misfolded/damaged proteins or specific substrates, such as cyclins. To test this hypothesis, we used another model proteasome substrate, GFP-von Hippel-Lindau (VHL). When expressed in yeast, the mammalian VHL protein cannot fold correctly and is polyubiquitinated and targeted to the proteasome (29). VHL thus provides a marker for ubiquitin-dependent degradation. Consistent with this model, we found that proteasome inhibitors caused GFP-VHL to accumulate in zinc-replete wild-type cells (Fig. 5*C*). In zinc-replete conditions, little GFP-VHL accumulated in either *ubi4*Δ or *ubi4 rpt2*^{E301K} mutants (Fig. 5, *D* and *E*), indicating that replete cells efficiently ubiquitinated and degraded this substrate. These results indicate that even though *rpt2*^{E301K} mutant proteasomes have a reduced ability to degrade mODC they retain sufficient activity to effectively degrade ubiquitinated VHL-GFP. Zinc-limited *ubi4*Δ cells had an increased level of GFP-VHL, but this effect was reversed in zinc-deficient *ubi4*Δ *rpt2*^{E301K} cells. Because

the *rpt2*^{E301K} mutation restored ubiquitin content of *ubi4*Δ, these results are consistent with the ubiquitination of VHL being the rate-limiting step in its degradation. Thus, our observations are consistent with *rpt2*^{E301K} suppressing *ubi4*Δ by increasing the ubiquitin supply with a resulting restoration of ubiquitin-dependent proteasomal degradation.

In addition to a decreased rate of ubiquitin degradation by the proteasome, increased expression of the Ub-RP genes could also contribute to the elevated ubiquitin in *ubi4*Δ *rpt2*^{E301K} cells. To test this hypothesis, we used RT-qPCR to determine the effect of *rpt2*^{E301K} on *RPL40A*, *RPL40B*, and *RPS31* expression (Fig. 3*B*). In zinc-replete conditions, *ubi4*Δ *rpt2*^{E301K} had reduced expression of the Ub-RP genes likely because of the slower growth rate caused by the *rpt2* mutation. In zinc-deficient cells, the *rpt2*^{E301K} mutation caused ~3-fold increases in expression of the Ub-RP fusion genes relative to their expression in *ubi4*Δ single mutants. Thus, increased expression of Ub-RP fusion genes during zinc deficiency may also contribute to the overall increase in ubiquitin levels observed in the suppressed strain.

*Protein Homeostasis Is Disrupted in Zinc-deficient ubi4*Δ *Mutants*—The *ubi4*Δ mutation inhibited degradation of a ubiquitin-dependent proteasome substrate (GFP-VHL) in zinc-deficient cells but not in replete cells. This result suggested that, in zinc-deficient *ubi4*Δ mutants, protein quality control may be disrupted. Because many proteasome substrates are damaged or misfolded proteins, loss of proteasome activity might increase the accumulation of these substrates. To test this hypothesis, we first analyzed the activity of the heat shock-regulated transcription factor Hsf1, which responds to unfolded protein accumulation. Changes in Hsf1 activity in response to zinc status and *UBI4* genotype were measured using a synthetic HSE-lacZ reporter gene (21). Reporter activity was strongly induced by a 1-h heat shock at 37° in both wild-type and *ubi4*Δ zinc-replete cells (Fig. 5*F*). Activity was also induced by zinc deficiency but only in the *ubi4*Δ strain, consistent with this mutation increasing unfolded protein accumulation.

Additional evidence for the accumulation of unfolded proteins in *ubi4*Δ came from analysis of Hsp104-GFP aggregation. As previously reported (21), a GFP-tagged version of the disaggregase protein chaperone Hsp104 formed discrete foci within zinc-deficient cells lacking the Tsa1 protein chaperone (Fig. 5, *G* and *H*). These foci are thought to represent the association of Hsp104 with aggregates of misfolded proteins. Hsp104-GFP-marked foci were even more abundant in zinc-deficient *ubi4*Δ cells than in *tsa1*Δ, suggesting that *ubi4*Δ cells also accumulate aggregates of unstable proteins. Although *tsa1*Δ mutant cells primarily had one or two large foci per cell, zinc-limited *ubi4*Δ mutants tended to have multiple smaller foci (Fig. 5*G*). Together, these data are consistent with the hypothesis that substrates of the ubiquitin-dependent proteasomal degradation pathway instead accumulate and aggregate in zinc-deficient *ubi4*Δ cells.

UBI4 Gene Expression Is Induced by Zap1 in Zinc-deficient Conditions—In analyzing the effect of zinc status on *UBI4* expression, we found that this gene was highly induced in zinc-deficient cells (Fig. 3*B*). Because previous transcriptome analyses did not identify *UBI4* as a Zap1 target gene, we examined the mechanism of this induction more closely. Quantitative RT-PCR analysis of *UBI4* expression showed a rapid increase and then sustained expression over time as zinc-replete wild-type cells transitioned to deficient conditions (Fig. 6*A*). This response was kinetically similar to the induction observed for the well characterized Zap1 target genes *ADH4* and *ZRT3*. *UBI4* was previously shown to be a target of both the Hsf1 heat shock factor and the stress response factors Msn2 and Msn4 (30). However, genes known to be regulated by these other factors (*e.g. SSA3*, *CTT1*, and *DDR2*) were not highly induced in wild-type zinc-deficient cells (data not shown). These results prompted us to examine the *UBI4* gene for potential ZREs that are required for Zap1 binding and regulation. The upstream promoter region contains previously mapped HSE and stress response element sequences (STRE) required for regulation of *UBI4* by Hsf1 and Msn2/Msn4, respectively (Fig. 6*B*). No sequences similar to the ZRE consensus (5′-ACCTTNAAGGT-3′) were found in the upstream promoter region of *UBI4.* However, we did identify three instances of the sequence 5′-ACCTCTAGGGT-3′, which closely matched the consensus ZRE, within the *UBI4* coding region. These potential ZREs were located just downstream of the start of the third, fourth, and fifth ubiquitin repeats in the ORF. Despite complete conservation of the ubiquitin amino acid sequence between the repeats, no ZRE-related sequences were found in the first two ubiquitin repeats.

The presence of potential intragenic ZREs downstream and far distant from the upstream *UBI4* promoter suggested that alternative transcription start sites might be used during zinc deficiency. Therefore, sites of *UBI4* transcription initiation were determined using a modified RLM-RACE method to identify mRNA 5′-ends. Consistent with previous results (30), several transcription start sites were found upstream of the *UBI4* ORF in zinc-replete cells (Fig. 6*B*). In zinc-limited cells, we identified start sites within this upstream region but also observed novel transcription start sites within the ORF; most were located just downstream of the putative ZRE within the third ubiquitin repeat. To independently confirm the existence of these alternative transcripts and assess their relative abundance, we performed Northern blotting analysis using a strand-specific probe to the ~100-nucleotide *UBI4* 3′-UTR. Consistent with the transcription start site data, analysis of mRNA generated from the chromosomal *UBI4* gene in zinc-replete cells revealed a full-length ~1.5-kb mRNA (Fig. 6*C*). Zinc-deficient cells expressed the full-length transcript (1.5 kb) and shorter transcripts of ~0.5 kb. The size of the shorter transcripts detected with a 3′-UTR probe is consistent with the transcription start sites we mapped within the *UBI4* ORF. If translation begins at the methionine codon at the beginning of the fourth ubiquitin repeat, the short mRNA produced in zinc-deficient cells would encode two full ubiquitin monomers. We noted that the high abundance of the short transcripts as determined by Northern blotting analysis contrasts with the relatively small proportion of intragenic transcripts detected by RLM-RACE (Fig. 6*A*). This inconsistency is likely due to the homology shared between the ubiquitin repeats of *UBI4* and other ubiquitin genes as sequence reads that could not be

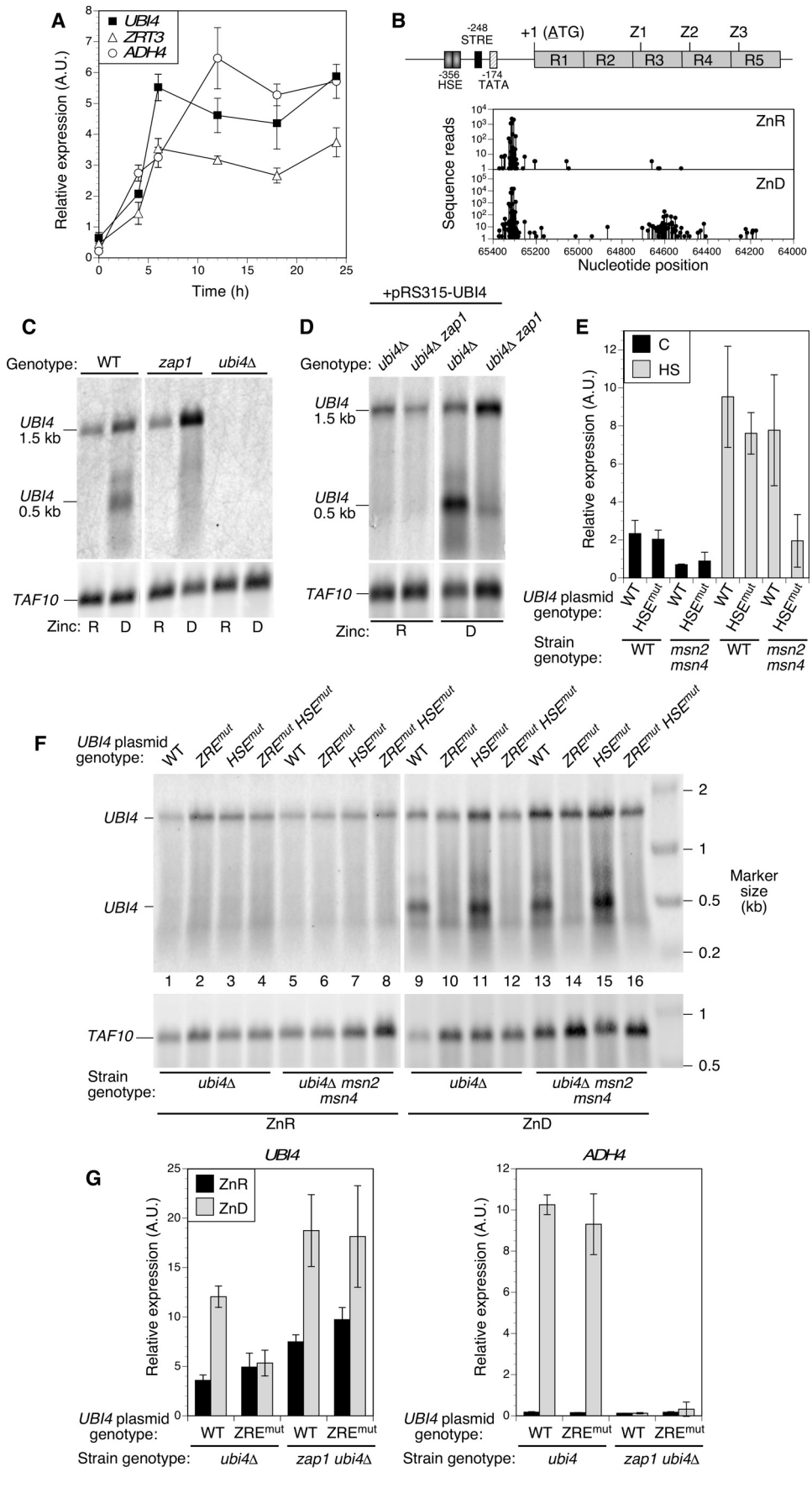
A
UBI4
ZRT3
ADH4
Relative expression (A.U.)
Time (h)
B
-248
STRE
+1 (ATG)
Z1
Z2
Z3
R1
R2
R3
R4
R5
-356
HSE
-174
TATA
ZnR
ZnD
Sequence reads
Nucleotide position
C
Genotype: WT zap1 ubi4Δ
UBI4
1.5 kb
UBI4
0.5 kb
TAF10
Zinc: R D R D R D
+pRS315-UBI4
D
Genotype: ubi4Δ ubi4Δ zap1 ubi4Δ ubi4Δ zap1
UBI4
1.5 kb
UBI4
0.5 kb
TAF10
Zinc: R D
E
C
HS
Relative expression (A.U.)
UBI4 plasmid genotype: WT HSEmut WT HSEmut WT HSEmut WT HSEmut
Strain genotype: WT msn2 msn4 WT msn2 msn4
F
UBI4 plasmid genotype: WT ZREmut HSEmut ZREmut HSEmut
UBI4
UBI4
Marker size (kb)
2
1
0.5
0.2
1 2 3 4 5 6 7 8 9 10 11 12 13 14 15 16
TAF10
1
0.5
Strain genotype: ubi4Δ ubi4Δ msn2 msn4 ubi4Δ ubi4Δ msn2 msn4
ZnR
ZnD
G
UBI4
ADH4
ZnR
ZnD
Relative expression (A.U.)
UBI4 plasmid genotype: WT ZREmut WT ZREmut
Strain genotype: ubi4Δ zap1 ubi4Δ
UBI4 plasmid genotype: WT ZREmut WT ZREmut
Strain genotype: ubi4 zap1 ubi4Δ

unambiguously assigned to a single genomic site were filtered out during the RLM-RACE analysis.

To assess the role of Zap1 in *UBI4* regulation, we examined the mRNA produced by chromosomal *UBI4* in a *zap1*Δ mutant strain (Fig. 6*C*). Short transcripts were absent from *zap1*Δ cells, indicating that Zap1 was required for their production. A similar effect was seen when comparing *ubi4*Δ and *ubi4*Δ *zap1*Δ strains expressing *UBI4* from a plasmid (Fig. 6*D*). To determine whether production of the short *UBI4* transcripts was dependent on the ZRE-like sequences, we examined the effect of mutating and inactivating all three of the potential ZREs within the *UBI4* ORF. Codon-synonymous mutations were made to disrupt Zap1 binding without altering the ubiquitin protein sequence; we refer to this allele as $ubi4^{ZREmut}$. In *ubi4*Δ mutants, a plasmid bearing a wild-type copy of *UBI4* produced the full-length mRNA in zinc-replete and -deficient cells and both the long and short transcripts under zinc-deficient conditions (Fig. 6*F*, *lanes 1* and *9*). In contrast, the *ubi4*Δ strain complemented with a $ubi4^{ZREmut}$ plasmid produced only the full-length transcript independently of the zinc supply (Fig. 6*F*, *lanes 2* and *10*). These results indicated that expression of the 0.5-kb mRNA is completely dependent on Zap1 activation, whereas the full-length transcript is Zap1- and ZRE-independent.

A previous report suggested that stress response genes may be activated by zinc deficiency via the Msn2/4 transcription factors (31). To determine whether either Msn2/Msn4 or the heat shock factor Hsf1 play a role in regulating *UBI4* in response to zinc supply, we generated an allele in which the Hsf1 binding site (HSE) was deleted from the *UBI4* promoter ($ubi4^{HSEmut}$). Consistent with previous reports (30), we showed that the response of the *UBI4* promoter to heat stress was mediated independently by both Hsf1 and Msn2/Msn4 transcription factors; the $ubi4^{HSEmut}$ allele did not abolish the heat shock response in a wild-type strain, and the heat shock response of the normal *UBI4* promoter was not diminished in an *msn2 msn4* double mutant (Fig. 6*E*). However, the *UBI4* heat shock response was greatly decreased when the $ubi4^{HSEmut}$ promoter mutant was tested in an *msn2 msn4* strain.

Induction of the *UBI4* short transcripts in response to zinc deficiency was solely dependent on the ZREs; neither mutation of the *UBI4* HSE nor mutation of the Msn2/Msn4 factors had any effect on its abundance (Fig. 6*F*, *lane 9 versus lanes 11*, *13*, and *15*). From these data, we conclude that induction of *UBI4* in low zinc is mediated by Zap1 via interaction with the intragenic ZREs, and there is little if any contribution to zinc-responsive regulation by other stress-responsive factors binding to the upstream promoter. An analysis of total *UBI4* gene expression using RT-qPCR confirmed that the induction seen in zinc-deficient cells was eliminated by mutation of the intragenic ZRE sequences (Fig. 6*G*). In *zap1* mutant cells, *UBI4* induction occurs during zinc limitation, but this effect is no longer dependent on the ZREs. This result is consistent with our previous observation that Hsf1 activity is increased in zinc-deficient *zap1* mutants, which experience a much greater degree of stress than do wild-type cells (32).

Zap1-mediated Regulation of UBI4 Is Critical for Growth of zinc-deficient Cells—The observations that *UBI4* was essential for growth in zinc-deficient conditions and regulated by an intragenic Zap1-responsive promoter suggested that the transcripts produced during zinc deficiency would be functional and important for survival in low zinc. To test these predictions directly, we first determined whether the short transcripts alone were capable of supporting the growth of a *ubi4*Δ mutant in zinc-deficient conditions. Two plasmids were constructed to express either the full-length mRNA or a short intragenic transcript, both with their native 5′-UTRs, from the *GAL1* promoter. To drive *UBI4* expression in glucose-containing medium, the *GAL1* promoter was induced using the pGEV system (33). RT-qPCR analysis showed that both short and long transcripts were expressed in zinc-deficient cells (data not shown), and both effectively complemented the *ubi4*Δ growth defect in low zinc (Fig. 7*A*). This result indicates that the short *UBI4* mRNA is indeed translated. The short transcript complemented less effectively than did the long transcript, and this effect is likely due to its encoding only two ubiquitin repeats, leading to a proportional reduction in ubiquitin produced.

FIGURE 6. **Zap1 induces *UBI4* expression in zinc-deficient cells via an intragenic promoter.** *A*, *UBI4* induction parallels Zap1 target gene expression in zinc-deficient conditions. Log phase cultures of wild-type and *ubi4*Δ mutant cells grown in zinc-replete medium (LZM + 100 μM $ZnCl_2$) were used to inoculate zinc-deficient medium at time 0 (LZM + 1 μM $ZnCl_2$). Cells were harvested at the indicated times, and expression of the indicated genes was assayed by RT-qPCR. Each data point is the mean of three replicates, and the *error bars* denote ±1 S.D. *B*, location of potential Zap1 binding sites (ZREs) and transcription start sites in *UBI4*. The structure of the *UBI4* gene is shown with its previously mapped promoter elements for Hsf1 (HSE)- and Msn2/Msn4 (*STRE*)-dependent regulation and TATA box. *R1–R5* represent the ubiquitin repeats, and the locations of the potential intragenic ZREs are marked (*Z1–Z3*). The graphs below show the transcription start sites mapped by RLM-RACE using mRNA from zinc-replete (*ZnR*; LZM + 100 μM $ZnCl_2$) and zinc-deficient (*ZnD*; LZM + 1 μM $ZnCl_2$) cells. *C* and *D*, short 0.5-kb *UBI4* transcripts are dependent on zinc supply and Zap1. Northern blotting analysis of *UBI4* expressed from the chromosomal locus (*C*) or a *UBI4* plasmid bearing the full promoter (pRS315-UBI4; *D*) is shown. For *C*, wild-type, *zap1*Δ, and *ubi4*Δ haploid strains were transformed with pGK-ZRT1 to allow growth of *zap1*Δ mutants in low zinc and then grown in zinc-replete (*R*; LZM + 100 μM $ZnCl_2$) or zinc-deficient (*D*; LZM + 1 μM $ZnCl_2$) conditions prior to RNA extraction. For *D*, *zap1*Δ (CWM260) and *zap1*Δ *ubi4*Δ (CWM276) strains were transformed with both pRS315-UBI4 and pGK-ZRT1 prior to growth in zinc-deficient or -replete medium and RNA extraction. For *C* and *D*, *UBI4* mRNA was detected using a probe specific for the 3′-UTR, and *TAF10* was also detected as a loading control. *E*, mutation of the *UBI4* HSE blocks *UBI4* induction by heat shock but only in an *msn2*Δ *msn4*Δ mutant background. Wild-type (BY4741) or *msn2*Δ *msn4*Δ (DBY9435) strains were transformed with pRS315-UBI4 (wild-type *UBI4*) or pRS315-$UBI4^{HSEmut}$ (HSE mutant). Cells were grown to log phase at 25 °C in SD medium or subjected to heat shock (*HS*; 20 min at 39 °C) before harvesting. Total RNA was isolated and assayed for *UBI4* expression using RT-qPCR. Each data point is the mean of three replicates, and the *error bars* denote ±1 S.D. *F*, the *UBI4* ZRE is essential for production of intragenic transcripts. Yeast strains *ubi4*Δ (CWM260) and *ubi4*Δ *msn2*Δ *msn4*Δ (CWM274) were transformed with either the wild-type *UBI4* plasmid (pRS315-UBI4), a plasmid in which the three intragenic ZREs were mutated (pRS315-$UBI4^{ZREmut}$), the HSE mutant plasmid (pRS315-$UBI4^{HSEmut}$), or a plasmid in which both the ZREs and the HSE were mutated (pRS315-$UBI4^{HSEmutZREmut}$). Cells were grown and analyzed by Northern blotting as described for *C* and *D*. *G*, the ZREs are required for *UBI4* induction in zinc deficiency. Mutant *ubi4*Δ (CWM260) and *ubi4*Δ *zap1*Δ (CWM276) cells were transformed with pGK-ZRT1 together with either the wild-type *UBI4* plasmid (pRS315-UBI4) or the ZRE mutant plasmid (pRS315-$UBI4^{ZREmut}$). Cells were grown to log phase in zinc-replete (*ZnR*; LZM + 100 μM $ZnCl_2$) or zinc-deficient (*ZnD*; LZM + 1 μM $ZnCl_2$) medium prior to RNA extraction. Quantitative RT-PCR was used to measure total *UBI4* transcripts using primers specific to the fifth ubiquitin repeat that is present in both full-length and short transcripts. A Zap1 target gene (*ADH4*) was also detected as a positive control for loss of Zap1 function. Each data point is the mean of three replicates, and the *error bars* denote ±1 S.D. *A.U.*, arbitrary units.

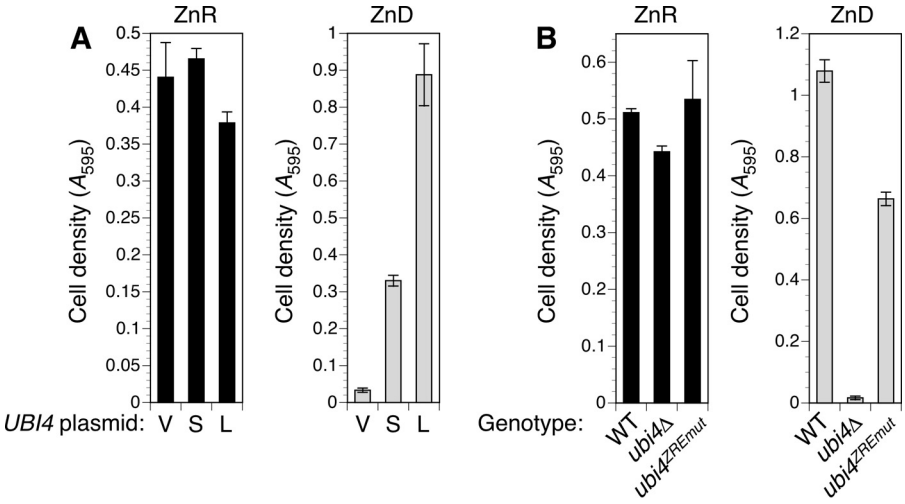

FIGURE 7. **Zap1-dependent regulation of *UBI4* is important for adaptation to zinc deficiency.** *A*, a short *UBI4* transcript generated from the *GAL1* promoter complemented *ubi4*Δ in low zinc. The *ubi4*::*KanMX4* strain was co-transformed with pGEV-HIS3 and either the empty vector pRS316-GAL1 (*V*) or pGAL1-UBI4S (*S*) or pGAL1-UBI4L (*L*) plasmids encoding short and long *UBI4* transcripts, respectively. Strains were grown in SD medium prior to inoculating cultures of zinc-deficient (*ZnD*; LZM + 1 μM zinc) or -replete (*ZnR*; LZM + 100 μM zinc) medium to low initial densities. LZM also contained 1 μM β-estradiol to induce the *GAL1* promoter. Cultures were grown for 15 (replete) or 63 h (deficient) before recording cell densities. *B*, mutation of the ZREs in the *UBI4* coding sequence caused poor growth in zinc-deficient conditions. Wild-type (CWM286), *ubi4*Δ (CWM281), and *ubi4*^{ZREmut} (CWM285) strains were cultured in SD medium prior to inoculating zinc-deficient (*ZnD*; LZM + 0.5 μM zinc) or zinc-replete (*ZnR*; LZM + 100 μM zinc) medium. Cell densities were determined after 16 (zinc-replete) or 65 h (zinc-deficient). Each data point is the mean of three replicates, and the *error bars* denote ±1 S.D.

To test the importance of Zap1-mediated *UBI4* induction to growth of zinc-deficient cells, we constructed a strain in which the endogenous *UBI4* locus was replaced with the ZRE mutant allele (*ubi4*^{ZREmut}). Integrating *UBI4* into the genome instead of using a plasmid ensured that the gene would not be overexpressed as a consequence of higher copy number. Comparison of wild-type, *ubi4*Δ, and *ubi4*^{ZREmut} cell growth in zinc-deficient conditions revealed that although the *ubi4*^{ZREmut} strain grew better than the *ubi4*Δ null mutant it grew less well than cells with the Zap1-responsive wild-type *UBI4* gene (Fig. 7*B*). All three strains grew equally well in a zinc-replete medium. These observations confirm that the unconventional activation of *UBI4* expression in low zinc via an intragenic promoter is essential for its full function in zinc-deficient cells.

Discussion

In this report, we provide strong evidence that *UBI4*, an essential gene for zinc-deficient cells, is a novel Zap1 target gene. For all previously described target genes, Zap1 activates gene expression from upstream promoters in response to zinc-limiting conditions. Consistent with its regulation by Zap1, total *UBI4* mRNA levels are induced by ~5-fold in zinc-deficient cells. Surprisingly, however, we found that the induction in zinc-limited cells is primarily driven by the increased abundance of truncated mRNAs initiating within the third ubiquitin repeat, a location over 700 base pairs downstream of the major start site for full-length transcripts. The full-length *UBI4* mRNA encodes five tandem copies of the ubiquitin protein. The truncated *UBI4* mRNA encodes two complete ubiquitin repeats and hence can still contribute significantly to the total ubiquitin supply. Also consistent with its regulation by Zap1, we found that mutation of three potential Zap1 binding sites (ZREs) found within the *UBI4* ORF blocks induction in low zinc. We have not yet determined which of the three potential ZREs mediates the increased *UBI4* expression, but it is most likely that the ZRE in the third ubiquitin repeat, which is just upstream of the major site for intragenic initiation, plays the primary role.

UBI4 is known to be a stress-inducible gene that is up-regulated under heat stress by the Hsf1 transcriptional activator. In addition, the Msn2 and Msn4 stress-responsive transcription factors have been shown to induce *UBI4* expression in response to heat and other stresses. These factors activate *UBI4* expression from binding sites located in the upstream promoter region flanking the ORF. A previous report indicated that the Msn2/4 factors are activated by zinc deficiency (31), suggesting these factors might be responsible for *UBI4* induction. However, we showed here that neither Msn2/4 nor Hsf1 play a major role in activating *UBI4* in zinc-limited wild-type cells and that Zap1 is primarily responsible for this effect.

There are several examples of alternative transcription start sites close to initiation codons that produce isoforms of gene products with different properties. For example, alternative start sites dictate the production of secreted and cytosolic forms of invertase generated by the *SUC2* gene (34) and cytosolic and mitochondrial isozymes of the Fum1 fumarase (35). Analogously, alternative start sites near the 5′-end of the *KAR4* ORF generate isoforms with different degrees of protein stability, thereby controlling protein accumulation under different conditions (36). However, these examples involve differences in transcription start site selection driven by flanking promoter elements. Activation of *UBI4* by Zap1 is unusual in that it apparently occurs from an intragenic promoter. Intragenic promoters are rare in *Saccharomyces* and other organisms. For example, Arribere and Gilbert (37) found that only about 1% of transcription start sites in yeast were located further than 100 nucleotides downstream of initiation codons, which quantitatively demonstrates the rarity of intragenic promoters in yeast. Intragenic promoters are likely to be rare due to various mech-

anisms repressing cryptic transcriptional initiation within transcribed regions. For example, transcribing RNA polymerase II recruits histone deacetylases, such as the Rpd3S complex, which deacetylate histones in the transcribed regions to maintain chromatin packing and inhibit intragenic transcription initiation (38). Similarly, the Spt6 histone chaperone represses intragenic transcription by binding to transcribing RNA polymerase II and maintaining nucleosome density in these regions (39, 40). Mutations that disrupt these activities lead to increased levels of intragenic transcription.

The existence and effectiveness of mechanisms that suppress cryptic initiation raise the question of how Zap1 is able to activate an intragenic *UBI4* promoter under zinc-limiting conditions. Specifically, does Zap1 have a mechanism to overcome repressive chromatin structure to initiate transcription? Alternatively, could repressive chromatin modifications be altered by the condition of zinc deficiency itself, thereby allowing Zap1 to bind? Supporting the latter hypothesis, we note that although a constitutive Zap1 allele did not activate the intragenic *UBI4* promoter in zinc-replete cells it did activate other Zap1 targets from upstream promoters (16) (data not shown). This result suggests that other factors or conditions altered by zinc status are required along with active Zap1 to turn on the intragenic *UBI4* promoter in zinc-limited cells. For example, zinc deficiency could decrease the activity of zinc-dependent histone deacetylases, such as the Rpd3S complex, thereby opening up chromatin structure for binding of Zap1. Therefore, an attractive hypothesis is that decreased deacetylase function is a requirement for activation of the intragenic *UBI4* promoter in zinc-limited cells.

An intriguing question is whether an intragenic promoter has some advantage for *UBI4* expression over regulation via an upstream flanking promoter. Although we can offer no compelling answers to this question, we can suggest how this intragenic promoter arose evolutionarily. The highly invariant amino acid sequence of ubiquitin contains the peptide TLEV. The possible codons that encode this peptide (ACN (C/T)TN GA(A/G) GTN) match the ZRE consensus at six of its 10 conserved positions and are constrained at two other positions such that one of two possible nucleotides match the ZRE consensus (underlined). Thus, ZREs arising through random mutation at these sites in the *UBI4* ORF seem highly likely. Moreover, because of the polyubiquitin structure of the *UBI4* gene product, once intragenic Zap1 binding sites arose, production of full-length ubiquitin protein from truncated mRNA could occur and, as we have shown, provide cells with a fitness advantage under zinc-limiting conditions.

We have shown that the *UBI4* gene is the major source of ubiquitin in zinc-limited cells. Although *UBI4* expression increases due to Zap1 regulation, expression of the three other ubiquitin genes, *RPL40A*, *RPL40B*, and *RPS31*, decreases. Thus, in wild-type cells, up-regulation of *UBI4* by Zap1 compensates for the effect of reduced growth rate on Ub-RP gene expression. In a *ubi4*Δ mutant, we propose that a downward spiral of effects occurs that ultimately leads to arrested growth. Zinc deficiency slows growth, which leads to decreased Ub-RP gene expression, which further slows growth and Ub-RP expression until ubiquitin supplies are inadequate for viability. In contrast, the *rpt2*^{E301K} mutation may suppress the *ubi4*Δ growth defect through an opposite, upward spiral of effects. Degradation of ubiquitin by the proteasome during its normal function gives this protein a half-life of as low as 2 h under stress conditions (26). Although we have not measured the half-life of ubiquitin in zinc-deficient cells, proteasomal degradation of ubiquitin is still likely to be a significant factor in dictating ubiquitin abundance. We hypothesize that competition occurs at the proteasome between degradation of ubiquitin along with its substrate *versus* release of ubiquitin by proteasome-associated deubiquitinases before substrate degradation occurs. A small decrease in the rate of proteasome activity could increase the residence time of the ubiquitin-substrate complex on the regulatory particle and thereby increase the likelihood of deubiquitination and ubiquitin release. The resulting small increase in ubiquitin levels would improve growth, which would then lead to more Ub-RP expression, still better growth, and so on. For this model to be true, the supply of ubiquitin and consequent rate of ubiquitination would have to be rate-limiting for substrate degradation rather than proteasomal degradation *per se*. The behavior of GFP-VHL in *ubi4*Δ and *ubi4*Δ *rpt2*^{E301K} mutants is consistent with this hypothesis. Alternatively, suppression of *ubi4*Δ by mutations affecting proteasome activity could result from changes in Ub-RP expression without altering ubiquitin degradation. Consistent with this hypothesis, proteasomal degradation of the Sfp1 transcription factor is required for repression of RP (and presumably Ub-RP) gene expression during nutrient limitation (41).

Zap1 activates the expression of ~80 genes in low zinc. By assessing the growth rates of mutants disrupted for these genes, we found a wide range of growth phenotypes in zinc-limiting medium from improved growth relative to wild-type cells to very poor growth. *UBI4* is clearly among the most important of the Zap1 target genes. A *ubi4*Δ mutant grew as poorly in low zinc as mutants lacking the Zrt1 high affinity zinc uptake transporter (the major pathway for zinc accumulation by zinc-deficient cells) or the Tsa1 peroxiredoxin/chaperone. Our previous analysis of Tsa1 suggested that zinc-limited cells were disrupted for protein homeostasis and suffered a toxic buildup of unfolded and misfolded proteins. We hypothesized that this disruption was due to the limited supply of zinc in these cells that is available for facilitating protein folding. In a zinc-limited cell, newly synthesized zinc-binding proteins would lack their needed cofactor and may misfold and aggregate. The chaperone activity of Tsa1 is critical for low zinc growth possibly because Tsa1 stabilizes accumulated apoproteins to facilitate their eventual metallation and folding.

The similarly severe phenotype of *ubi4*Δ mutants to that of *tsa1*Δ mutants suggests a critical function for *UBI4*. A complementary system to deal with zinc-related disruptions in protein homeostasis might be the ubiquitination and degradation of apoproteins by the proteasome. Consistent with this role, we found that the level of ubiquitin conjugates rises in zinc-limited wild-type cells, whereas free ubiquitin levels decrease (Fig. 3), suggesting that there is substantially more substrate for proteasomal degradation. Also consistent with this hypothesis, we noted that two assays for accumulated unfolded proteins were positive in zinc-deficient *ubi4*Δ cells, specifically induction of the heat shock factor-responsive HSE-lacZ reporter and the

formation of Hsp104-GFP foci. Lastly, we note that *ubr1*Δ mutants are also defective for zinc-limited growth (Fig. 1). Ubr1 is a ubiquitin ligase that is important for the ubiquitination of misfolded and damaged proteins to target them for proteasomal degradation (42, 43). These data all support the importance of the ubiquitin-proteasome system for maintenance of protein homeostasis when zinc supplies are inadequate.

Another possible explanation for the slow growth of *ubi4*Δ mutant cells in low zinc was suggested by studies of RNA polymerase I. Lee *et al.* (44) showed that RNA polymerase I subunit Rpa190 is ubiquitinated and stable under zinc-replete conditions but is deubiquitinated in zinc-limited cells, targeting it to the vacuole for degradation. Reduced ubiquitin supply in a zinc-deficient *ubi4*Δ mutant could result in a further decrease in Rpa190 and RNA polymerase I activity, potentially to levels insufficient to support even slow growth. Other potentially critical functions of ubiquitin in zinc-limited cells were suggested by the identity of ubiquitin metabolism genes required for growth in low zinc (Fig. 1). For example, mutants disrupted for the *BUL1* and *BRE5* genes showed very strong defects in zinc-limited growth. Bul1 is an arrestin-like adapter for the Rsp5 E3 ubiquitin ligase (45) that is known to recruit the Rsp5 ubiquitin ligase to amino acid transporters like Gap1 and Tat1, triggering their ubiquitination and subsequent endocytosis and degradation (46). Given this function, the low zinc growth defect of *bul1*Δ mutants could be due to aberrant regulation of plasma membrane transporter proteins. *BRE5* encodes a subunit of the Ubp3-Bre5 deubiquitinase complex. Mutation of *BRE5* disrupts a wide variety of functions including endoplasmic reticulum to Golgi trafficking (47), DNA damage repair (48), stress granule assembly (49), and ribophagy in response to nitrogen starvation (50). A recent proteome-wide analysis showed that the levels of over 400 proteins were affected in cells lacking the Ubp3 deubiquitinase subunit (51, 52). The diverse phenotypes of mutants lacking Ubp3-Bre5 complex activity suggest that a number of different Ub-dependent processes may normally contribute to the survival of cells in zinc-deficient conditions. Future studies will investigate both the proteasomal and non-proteasomal functions of ubiquitin in zinc-deficient cells.

Experimental Procedures

Yeast Media and General Methods—Yeast strains were routinely grown in rich medium, synthetic defined medium, or LZM as described previously (53). LZM contains 20 mM citrate and 1 mM EDTA to buffer pH and zinc availability. Glucose (2%) was the carbon source for all experiments. LZM + 1 μM $ZnCl_2$ was routinely used as the zinc-deficient condition, and LZM + 100 μM $ZnCl_2$ was used as the zinc-replete condition. To aid growth of S288c-derived mutant strains, LZM was routinely supplemented with amino acids and inositol (54). For some experiments, YPD medium was made deficient for iron by adding bathophenanthroline disulfonic acid or for copper by adding bathocuproine disulfonic acid. Fluorescence microscopy to detect Hsp104-GFP foci was performed as described previously (21).

Yeast Strain Construction—The yeast strains used in this work are isogenic to BY4743 (*MATa*/*MATα his3Δ1*/*his3Δ1 leu2Δ0*/*leu2Δ0 met15Δ0*/*MET15 lys2Δ0*/*LYS2 ura3Δ0*/*ura3Δ0*) or BY4741 (*MATa his3Δ0 leu2Δ0 met15Δ0 ura3Δ0*). Haploid and homozygous diploid *KanMX4*-marked deletion mutant strains of the yeast genome deletion collection (including haploid *zap1*Δ and *ubi4*Δ and all homozygous diploid mutant strains) were obtained from Invitrogen. Additional multiply marked mutant strains were generally derived from BY4741 single mutants via transformation (55). A *ubi4*::*HphMX4* strain (CWM260) was generated by transformation of the haploid *ubi4*::*KanMX4* with the hygromycin resistance gene excised from pAG32 (56). *pre1*^{DAmP} *ubi4*Δ and *pre6*^{DAmP} *ubi4*Δ (CWM278 and -279) were generated by transformation of BY4741 *pre1*^{DAmP}::*KanMX4* and *pre6*^{DAmP}::*KanMX4* haploid strains (GE Dharmacon) (57) with the *ubi4*Δ::*HphMX4* marker, amplified from genomic DNA of CWM260. The same method was used to construct CWM274 (*ubi4*Δ *msn2*Δ *msn4*Δ) from DBY9435 (BY4741 *msn2*::*KanMX4 msn4*Δ::*URA3*) (58) and to construct CWM276 (*ubi4*Δ *zap1*Δ) from BY4741 *zap1*Δ::*KanMX4*. Construction of a *LEU2-ubi4*^{ZREmut} strain (CWM285) was achieved in two steps. First, the *HphMX4* marker in CWM260 was replaced with a *klURA3* marker, constructed by using PCR to add 80 bp of terminal *HphMX4* homology to the *klURA3* gene from the pCORE plasmid (59). The resulting strain (CWM281) was transformed with a fragment encompassing the *LEU2* selectable marker and *ubi4*^{ZREmut} gene. This construct was amplified from the pRS315-UBI4^{ZREmut} plasmid, incorporating homology to the region flanking the *UBI4* locus at the *LEU2* end of the construct. Clones that correctly integrated the *LEU2-ubi4*^{ZREmut} allele at the *ubi4*::*klURA3* locus were identified via loss of *URA3* function and confirmed by sequencing PCR products amplified from *UBI4*. An isogenic *LEU2-UBI4* wild-type strain (CWM286) was similarly constructed by replacing *klURA3* with a wild-type *LEU2-UBI4* fragment amplified from pRS315-UBI4. CWM280 (*rpt2*^{E310K} *ubi4*::*KanMX4*) was isolated from an ethyl methanesulfonate-mutagenized population of BY4741 *ubi4*::*KanMX4* as described below.

Plasmids—Plasmids pHSE-lacZ (21), pHSP104-GFP (21), pGK-ZRT1 (15), p415-GFP-FLAG-mODC (28), and pESC-LEU-GALp-GFP-VHL (60) were described previously. Novel plasmids were generally constructed by PCR and gap repair in yeast, and all constructs were verified by sequencing. pRS316-RPT2 was constructed by amplifying a fragment of chromosome IV (bases 437417–439857) from genomic DNA of BY4743 using oligonucleotides with flanking homology to the pRS316 vector to allow cloning via gap repair in yeast. pRS315-UBI4 and pRS316-UBI4 were constructed using the same strategy. pRS315-UBI4 includes bases 63263–66063 of chromosome XII, and pRS316-UBI4 includes bases 63538–66203. pRS315-UBI4^{HSEmut} was constructed by amplifying two fragments of the *UBI4* gene using primers designed to generate an overlap at the previously identified HSE sequence (30). The 34-bp overlapping region included a mutated version of the HSE (5′-ATATCCCGGGATATCCTACGACTT-3′), designed to eliminate recognition by Hsf1. Both fragments were combined and cloned by recombination with gapped pRS315 in yeast. The pRS315-pUBI4^{ZREmut} plasmid was constructed in part by manufacture of a synthetic mutant gene. A 1.7-kb fragment of the *UBI4* coding sequence was synthesized (Genewiz) to incorporate silent mutations in all three putative ZRE

sequences (5′-ACCCTAGAGGT-3′), converting them to the predicted inactive sequence (5′-ACATTGGAAGT-3′). pRS315-UBI4 was digested with BglII and NruI to remove a portion of *UBI4* containing the wild-type ZRE sequences and the mutant fragment introduced via gap repair. The pRS315-UBI4^{HSEmutZREmut} plasmid was constructed by using the same strategy to introduce the mutant ZRE fragment into the pRS315-UBI4^{HSEmut} plasmid. Plasmids expressing *UBI4* transcripts from the *GAL1* promoter (pGAL1-UBI4L and pGAL1-UBI4S) were constructed by amplifying the complete or partial coding sequence and terminator region of *UBI4* from genomic DNA using primers that included flanking homology to the pRS316-GAL1 plasmid to allow their introduction by gap repair. These constructs were designed to produce mRNA identical to abundant long and short native transcripts. The short transcript corresponds to initiation at nucleotide 64602 of chromosome XII. Expression of *GAL1* promoter-driven constructs in glucose medium was achieved using the pGEV system (33). Cells were co-transformed with the *GAL1*-driven construct and plasmid pGEV, a hybrid activator protein containing the Gal4 DNA-binding domain, the hormone-responsive domain of the estrogen receptor, and the VP16 activation domain. Treatment of pGEV-containing cells with 1 μM β-estradiol drove high levels of expression as assayed by quantitative RT-PCR (data not shown).

Identification of the rpt2^{E301K} Suppressor Mutation—The BY4741 *ubi4*::*KanMX4* strain was grown in YPD and mutagenized to 50% viability with ethyl methanesulfonate according to standard protocols (61). Pools of 4.5×10^5 viable mutant cells were outgrown in SD medium until stationary phase and used to inoculate LZM + 1 μM $ZnCl_2$ to a starting A_{600} of 0.01. These cultures were incubated at 30 °C, and cell density was monitored for 2–14 days. Cultures that reached an A_{600} of at least 0.3 were plated on SD medium to isolate individual colonies and then retested by growth in LZM + 1 μM $ZnCl_2$ to identify strongly suppressed strains. Selected clones were mated with an isogenic *ubi4*Δ haploid, and diploids were grown in low zinc to identify recessive suppressor mutations for further analysis. The *rpt2^{E301K}* suppressor mutation was identified from a selected suppressed strain (CWM280) by using pooled linkage analysis and whole genome sequencing essentially as described previously (21). As homozygous diploid *ubi4*Δ strains have a sporulation defect (62), the *ubi4* mutation was complemented with the pRS316-UBI4 plasmid. Haploid segregants were cured of the ubiquitin plasmid by growth on 5-fluoroorotic acid medium, and scored for the suppressor gene by growth in LZM + 1 μM $ZnCl_2$. For Illumina sequencing of pooled segregants, genomic DNA was isolated from pools of 15 suppressed haploids and 15 nonsuppressed haploids, respectively. The identification of the *rpt2^{E301K}* mutation as the suppressor was confirmed by complementation with a plasmid clone of wild-type *RPT2* (data not shown).

Analysis of Relative Growth by Flow Cytometry—The BY4743 wild-type strain was transformed with an integrating vector that expresses GFP from the strong *TEF2* promoter (57), which was targeted to the *his3Δ0* allele. GFP-tagged wild-type and untagged isogenic mutant strains were grown overnight to exponential phase (A_{600} = 0.5) in YPD, mixed in approximately equal numbers, and used to inoculate 5-ml cultures of LZM + 1 or 100 μM $ZnCl_2$ to a starting A_{600} of 0.00375. Cultures were allowed to reach an A_{600} of 1.0, then used to inoculate fresh cultures of the same medium to an A_{600} of 0.0075, and grown to a final A_{600} of 1.0 for a total of 15 generations. Approximately 20,000 total cells per culture were analyzed by flow cytometry using a FACSCalibur flow cytometer (BD Biosciences). A 530/30 filter was used for measuring GFP fluorescence, and a 585/42 filter was used to detect autofluorescence exhibited by both tagged and untagged cells. GFP-expressing wild type cells were readily distinguished from untagged mutant cells. Control experiments determined that <1% of wild-type cells did not accumulate GFP, contributing little variability to mutant cell counts.

Protein Extraction and Immunoblotting—Yeast protein extracts were prepared using a TCA extraction protocol as described previously (21). SDS-PAGE and immunoblotting were conducted using the LI-COR Biosciences infrared dye detection system as described previously (21). For optimal detection of monoubiquitin and ubiquitin conjugates, immunoblots were boiled in purified water for 15 min prior to blocking. Antibodies used were anti-ubiquitin (Covance product P4D1, lot number EIIKF02325), anti-FLAG M2 (Sigma product F1804), anti-GFP (Roche Applied Science product 11814460001), and anti-Pgk1 (Abcam product 22C5D8, lot number GR166098). IRDye 680-labeled secondary anti-mouse antibody (product 680LT, lot number C30605-02) was obtained from LI-COR Biosciences.

RNA Extraction—Small scale isolation of yeast total RNA for RT-qPCR was performed using TRIzol reagent (Ambion) following the manufacturer's instructions. Cells of 5–25-ml log phase cultures were collected by centrifugation and frozen in liquid N_2 before processing. Large scale isolation of total RNA intended for Northern analysis was achieved using a hot phenol extraction method (63). Yeast cultures were grown to log phase in 25–200 ml of medium, collected by centrifugation, and frozen in liquid N_2 before processing.

Quantitative RT-PCR Analysis—For quantitative analysis of gene expression, 5 μg of total yeast RNA prepared using the TRIzol method was treated with 5 units of RQ1 RNase-free DNase (Promega) according to the manufacturer's instructions. DNase was removed by extraction with an equal volume of phenol:chloroform:isoamyl alcohol (25:24:1) and RNA was precipitated with ethanol. cDNA templates were generated from 0.5 μg of total RNA using qScript cDNA Supermix (Quanta) according to the manufacturer's instructions and then diluted 1:10 (for routine target detection) or 1:5000 (for detection of 18S rRNA). Primer pairs were selected with GenScript software and verified with Amplify software (64). The sequences of the primer pairs used were (5′–3′): CGACCCTTTGGAAGAGATGT and TCGAAAGTTGATAGGGCAGA (18S rRNA), CCAGAAGCTTTGTTCCATCC and ACGGACATCGACATCACACT (*ACT1*), ACCGTCAGAACAACTTTGCTT and GGCGTGCAGCAGATTTCACAA (*TAF10*), GCCTGTGCTTTGAAGGGTAT and CCTGCCAAGTATTCAGCGTA (*ADH4*), AGCAATTGGAAGACGGTAGAACC and ACAGTTGTACTTGGAAGCCAAAGC (*UBI1*), AGCAATTGGAAGACGGTAGAACTC and GGAAGCCAAGGCTTTCAAAGATGG (*UBI2*), ACAAGGTCGATGCTGAAGGT-

AAGG and ACCACAAGTTGGGTTGCTACATTC (*UBI3*), GAAGGTATTCCTCCAGACCAG and AGGACTGATCAGTTACCACCC (*UBI4*), CAACGCTTTCATTGCTTCC and GTCATCGTTGTGAGAAACTGG (*RPL1B*), and TGAGCGTTACTGCAGGGTTC and GTGCCTGAGCTATGGGACTG (*ZRT3*). RT-qPCR mixtures were prepared using Power SYBR Green 2× PCR Master Mix (Applied Biosystems), and reactions were performed using an ABI PRISM 7000 Sequence Detection System. To exclude the possibility of DNA contamination, control reactions were performed using RNA samples without reverse transcriptase treatment. The thermocycling program consisted of a 10-min step at 95 °C followed by 45 cycles of 15 s at 95 °C and 1 min at 58 °C. After completion of these cycles, the specificity of the reactions was checked by analysis of melting curve data. C_t values determined for target genes were converted to values of relative expression using the comparative C_t method ($2^{-\Delta\Delta Ct}$) (65). Target gene expression was calculated relative to the average C_t values for three control genes (*TAF10*, *ACT1*, and 18S rRNA) selected from multiple candidates for their highly stable expression under the conditions used in our experiments (data not shown).

Preparation of Antisense Probes for Northern Blotting Analysis—PCR fragments of the *UBI4* and *TAF10* genes were amplified from genomic DNA, introducing the T7 RNA polymerase promoter into the products in antisense orientation by inclusion in the downstream primer. Full probe primer sequences were (5′–3′): GTAACTGATCAGTCCTCGCA and AGTTAATACGACTCACTATAGGGAGGTCGGCTTATGTGCGTT (for *UBI4*) and ATGGATTTTGAGGAAGATTAC and AGTTAATACGACTCACTATAGGGACTAACGATAAAAGTCTGGGCG (for *TAF10*). Purified PCR product was used as template for synthesis of biotin-labeled RNA using T7 biotin labeling mixture (Roche Applied Science) and T7 polymerase (Roche Applied Science) according to the manufacturer's instructions. Labeled RNA was precipitated from the reaction mixture before use to separate it from residual biotin-labeled nucleotides and allow quantitation.

Northern Blotting Analysis—Northern blotting analysis of yeast mRNA samples was performed using a NorthernMax kit (Applied Biosystems) according to the manufacturer's instructions. Modifications to the protocol were incorporated to enable non-radioactive detection of biotin-labeled probes by using IRDye-labeled streptavidin with an Odyssey imager (LI-COR Biosciences). Briefly, poly(A) mRNA was purified from 250–500 μg of total RNA using a GenElute mRNA miniprep kit (Sigma); fractionated on a 1.2% agarose, formaldehyde gel; and transferred to nylon membranes (Biodyne B, Thermo Scientific) via capillary blotting. RNA was fixed to the membrane by baking at 80 °C for 30 min followed by cross-linking with 80 mJ of UV light. The membranes were prehybridized for 1 h with ULTRAhyb-Oligo solution (Ambion) at 60 °C and then incubated with fresh ULTRAhyb-Oligo solution containing a biotin-labeled antisense RNA probe (300 ng/ml) for 16 h at 60 °C. Low and high stringency washes were performed as detailed in the NorthernMax protocol using 68 °C for the high stringency wash step. Membranes were blocked with 1% SDS, Odyssey Blocking buffer solution (LI-COR Biosciences) for 1 h at room temperature and then incubated for 1 h with a 1:5000 dilution of steptavidin-800CW (LI-COR Biosciences product 925-32230) in the same buffer. Membranes were washed 3 × 5 min in a solution of 1× PBS, 0.1% Tween 20; washed once in 1× PBS, and detected wet using the 800 nm channel of the LI-COR Biosciences instrument. For size determination, a prestained RNA size marker (DynaMarker, Biodynamics) was fractionated in the gel and detected in the 680 nm channel. Before reprobing, Northern blots were stripped by treatment with boiling 1% SDS and reprocessed from the prehybridization stage.

Mapping of Transcription Start Sites by Deep-RACE—Transcription start sites were mapped genome-wide using the Deep-RACE method (66). In Deep-RACE, the gene-specific RLM-RACE method is adapted to a genome-wide analysis of mRNA 5′-ends. The full analysis of transcription start sites in zinc-deficient cells will be published elsewhere.[3] Wild-type (DY150) cells were grown in zinc-replete (LZM + 100 μM $ZnCl_2$) or zinc-deficient (LZM + 1 μM $ZnCl_2$) medium (six replicates each). Total RNA was isolated from each culture by the hot phenol method, and equal amounts of RNA from the replicate samples were pooled. Using the Ambion FirstChoice RLM-RACE kit, the RNA samples were treated first with calf intestinal alkaline phosphatase and then with tobacco acid pyrophosphatase followed by ligation with the 5′-RACE RNA adaptor (5′-GCUGAUGGCGAUGAAUACACUCUUUCCCUACACGACGCUCUUCCGAUCU-3′). Moloney murine leukemia virus reverse transcriptase was used to make cDNA with a random primer oligonucleotide (5′-CACGAGCGGTGACTGGAGTTCAGACGTGTGCTCTTCCGATCTNNNNNN-3′ where N = random nucleotides), and the cDNA products were then PCR-amplified using nested primer sets (first round outer primers (10 cycles), 5′-GCTGTGGCGATGAATACAC-3′ and 5′-CACGAGCGGTGACTGGAGTTC-3′; second round inner primers (15 cycles), 5′-ACACTCTTTCCCTACACGAC-3′ and 5′-GTGACTGGAGTTCAGACGTGTGC-3′) to generate a library of fragments containing the 5′-ends of mRNA. These fragments were sequenced by Illumina sequencing.

Identification of ZREs in the UBI4 Open Reading Frame—Potential ZREs in the *UBI4* gene were identified using Multiple EM for Motif Elicitation (MEME Suite 4.11.1) (67). A training set of the 1000-bp promoter sequences of 10 known Zap1 target genes (*YGL255W*, *ADH4*, *ZRT2*, *ZAP1*, *ZRT3*, *FET4*, *ZRG17*, *TSA1*, *VEL1*, and *ATG41*) was used to generate a ZRE position-specific scoring matrix using MEME. We then screened for ZRE-like sequences in the *UBI4* gene using Find Additional Motif Occurrences (FIMO) software and the ZRE position-specific scoring matrix.

Author Contributions—D. J. E. conceived and coordinated the study. K. K. performed the analysis in Figs. 1 and 5*F*. J. T. generated the data for Figs. 3*A*; 4, *B* and *D*; and 5, *A*–*E*. J. J. generated the data for Figs. 2 and 4, *A* and *C*. C. W. M. was responsible for Figs. 2*D*, 3*B*, 5*G*, 6, and 7. J. J., C. W. M., and D. J. E. were the primary contributors to the writing of the manuscript. All authors have reviewed the results and approved the final version of the manuscript.

[3] C. W. MacDiarmid, J. Taggart, J. Jeong, K. Kerdsomboon, and D. J. Eide, manuscript in preparation.

Acknowledgments—We thank Philip Coffino and Daniel Kaganovitch for providing plasmids and Mike Bucci for comments on the manuscript.

References

1. Vallee, B. L., and Auld, D. S. (1990) Zinc coordination, function, and structure of zinc enzymes and other proteins. *Biochemistry* **29,** 5647–5659
2. McCall, K. A., Huang, C., and Fierke, C. A. (2000) Function and mechanism of zinc metalloenzymes. *J. Nutr.* **130,** 1437S–1446S
3. Alberts, I. L., Nadassy, K., and Wodak, S. J. (1998) Analysis of zinc binding sites in protein crystal structures. *Protein Sci.* **7,** 1700–1716
4. Andreini, C., Banci, L., Bertini, I., and Rosato, A. (2006) Counting the zinc-proteins encoded in the human genome. *J. Proteome Res.* **5,** 196–201
5. Andreini, C., Bertini, I., Cavallaro, G., Holliday, G. L., and Thornton, J. M. (2009) Metal-MACiE: a database of metals involved in biological catalysis. *Bioinformatics* **25,** 2088–2089
6. Magonet, E., Hayen, P., Delforge, D., Delaive, E., and Remacle, J. (1992) Importance of the structural zinc atom for the stability of yeast alcohol dehydrogenase. *Biochem. J.* **287,** 361–365
7. Ganzhorn, A. J., and Plapp, B. V. (1988) Carboxyl groups near the active site zinc contribute to catalysis in yeast alcohol dehydrogenase. *J. Biol. Chem.* **263,** 5446–5454
8. Jeloková, J., Karlsson, C., Estonius, M., Jörnvall, H., and Höög, J. O. (1994) Features of structural zinc in mammalian alcohol dehydrogenase. Site-directed mutagenesis of the zinc ligands. *Eur. J. Biochem.* **225,** 1015–1019
9. Eide, D. J. (2009) Homeostatic and adaptive responses to zinc deficiency in *Saccharomyces cerevisiae. J. Biol. Chem.* **284,** 18565–18569
10. Lyons, T. J., Gasch, A. P., Gaither, L. A., Botstein, D., Brown, P. O., and Eide, D. J. (2000) Genome-wide characterization of the Zap1p zinc-responsive regulon in yeast. *Proc. Natl. Acad. Sci. U.S.A.* **97,** 7957–7962
11. Wu, C.-Y., Bird, A. J., Chung, L. M., Newton, M. A., Winge, D. R., and Eide, D. J. (2008) Differential control of Zap1-regulated genes in response to zinc deficiency in *Saccharomyces cerevisiae. BMC Genomics* **9,** 370
12. Zhao, H., Butler, E., Rodgers, J., Spizzo, T., Duesterhoeft, S., and Eide, D. (1998) Regulation of zinc homeostasis in yeast by binding of the *ZAP1* transcriptional activator to zinc-responsive promoter elements. *J. Biol. Chem.* **273,** 28713–28720
13. Bird, A. J., McCall, K., Kramer, M., Blankman, E., Winge, D. R., and Eide, D. J. (2003) Zinc fingers can act as Zn^{2+} sensors to regulate transcriptional activation domain function. *EMBO J.* **22,** 5137–5146
14. Herbig, A., Bird, A. J., Swierczek, S., McCall, K., Mooney, M., Wu, C.-Y., Winge, D. R., and Eide, D. J. (2005) Zap1 activation domain 1 and its role in controlling gene expression in response to cellular zinc status. *Mol. Microbiol.* **57,** 834–846
15. Frey, A. G., Bird, A. J., Evans-Galea, M. V., Blankman, E., Winge, D. R., and Eide, D. J. (2011) Zinc-regulated DNA binding of the yeast Zap1 zinc-responsive activator. *PLoS One* **6,** e22535
16. Bird, A. J., Gordon, M., Eide, D. J., and Winge, D. R. (2006) Repression of *ADH1* and *ADH3* during zinc deficiency by Zap1-induced intergenic RNA transcripts. *EMBO J.* **25,** 5726–5734
17. Iwanyshyn, W. M., Han, G. S., and Carman, G. M. (2004) Regulation of phospholipid synthesis in *Saccharomyces cerevisiae* by zinc. *J. Biol. Chem.* **279,** 21976–21983
18. Soto-Cardalda, A., Fakas, S., Pascual, F., Choi, H.-S., and Carman, G. M. (2012) Phosphatidate phosphatase plays role in zinc-mediated regulation of phospholipid synthesis in yeast. *J. Biol. Chem.* **287,** 968–977
19. Wu, C.-Y., Roje, S., Sandoval, F. J., Bird, A. J., Winge, D. R., and Eide, D. J. (2009) Repression of sulfate assimilation is an adaptive response of yeast to the oxidative stress of zinc deficiency. *J. Biol. Chem.* **284,** 27544–27556
20. Wu, C.-Y., Bird, A. J., Winge, D. R., and Eide, D. J. (2007) Regulation of the yeast *TSA1* peroxiredoxin by *ZAP1* is an adaptive response to the oxidative stress of zinc deficiency. *J. Biol. Chem.* **282,** 2184–2195
21. MacDiarmid, C. W., Taggart, J., Kerdsomboon, K., Kubisiak, M., Panascharoen, S., Schelble, K., and Eide, D. J. (2013) Peroxiredoxin chaperone activity is critical for protein homeostasis in zinc-deficient yeast. *J. Biol. Chem.* **288,** 31313–31327
22. Bagola, K., and Sommer, T. (2008) Protein quality control: on IPODs and other JUNQ. *Curr. Biol.* **18,** R1019–1021
23. North, M., Steffen, J., Loguinov, A. V., Zimmerman, G. R., Vulpe, C. D., and Eide, D. J. (2012) Genome-wide functional profiling identifies genes and processes important for zinc-limited growth of *Saccharomyces cerevisiae. PLoS Genet.* **8,** e1002699
24. Birkeland, S. R., Jin, N., Ozdemir, A. C., Lyons, R. H., Jr., Weisman, L. S., and Wilson, T. E. (2010) Discovery of mutations in *Saccharomyces cerevisiae* by pooled linkage analysis and whole-genome sequencing. *Genetics* **186,** 1127–1137
25. Schnall, R., Mannhaupt, G., Stucka, R., Tauer, R., Ehnle, S., Schwarzlose, C., Vetter, I., and Feldmann, H. (1994) Identification of a set of yeast genes coding for a novel family of putative ATPases with high similarity to constituents of the 26S protease complex. *Yeast* **10,** 1141–1155
26. Weissman, A. M., Shabek, N., and Ciechanover, A. (2011) The predator becomes the prey: regulating the ubiquitin system by ubiquitylation and degradation. *Nat. Rev. Mol. Cell Biol.* **12,** 605–620
27. Rivett, A. J., Mason, G. G., Thomson, S., Pike, A. M., Savory, P. J., and Murray, R. Z. (1995) Catalytic components of proteasomes and the regulation of proteinase activity. *Mol. Biol. Rep.* **21,** 35–41
28. Hoyt, M. A., Zhang, M., and Coffino, P. (2003) Ubiquitin-independent mechanisms of mouse ornithine decarboxylase degradation are conserved between mammalian and fungal cells. *J. Biol. Chem.* **278,** 12135–12143
29. McClellan, A. J., Scott, M. D., and Frydman, J. (2005) Folding and quality control of the VHL tumor suppressor proceed through distinct chaperone pathways. *Cell* **121,** 739–748
30. Simon, J. R., Treger, J. M., and McEntee, K. (1999) Multiple independent regulatory pathways control *UBI4* expression after heat shock in *Saccharomyces cerevisiae. Mol. Microbiol.* **31,** 823–832
31. Gauci, V. J., Beckhouse, A. G., Lyons, V., Beh, E. J., Rogers, P. J., Dawes, I. W., and Higgins, V. J. (2009) Zinc starvation induces a stress response in *Saccharomyces cerevisiae* that is mediated by the Msn2p and Msn4p transcriptional activators. *FEMS Yeast Res.* **9,** 1187–1195
32. Frey, A. G., and Eide, D. J. (2011) Roles of two activation domains in Zap1 in the response to zinc deficiency in *Saccharomyces cerevisiae. J. Biol. Chem.* **286,** 6844–6854
33. Louvion, J. F., Havaux-Copf, B., and Picard, D. (1993) Fusion of GAL4-VP16 to a steroid-binding domain provides a tool for gratuitous induction of galactose-responsive genes in yeast. *Gene* **131,** 129–134
34. Carlson, M., and Botstein, D. (1982) Two differentially regulated mRNAs with different 5′ ends encode secreted and intracellular forms of yeast invertase. *Cell* **28,** 145–154
35. Wu, M., and Tzagoloff, A. (1987) Mitochondrial and cytoplasmic fumarases in *Saccharomyces cerevisiae* are encoded by a single nuclear gene *FUM1. J. Biol. Chem.* **262,** 12275–12282
36. Gammie, A. E., Stewart, B. G., Scott, C. F., and Rose, M. D. (1999) The two forms of karyogamy transcription factor Kar4p are regulated by differential initiation of transcription, translation, and protein turnover. *Mol. Cell. Biol.* **19,** 817–825
37. Arribere, J. A., and Gilbert, W. V. (2013) Roles for transcript leaders in translation and mRNA decay revealed by transcript leader sequencing. *Genome Res.* **23,** 977–987
38. Carrozza, M. J., Li, B., Florens, L., Suganuma, T., Swanson, S. K., Lee, K. K., Shia, W. J., Anderson, S., Yates, J., Washburn, M. P., and Workman, J. L. (2005) Histone H3 methylation by Set2 directs deacetylation of coding regions by Rpd3S to suppress spurious intragenic transcription. *Cell* **123,** 581–592
39. DeGennaro, C. M., Alver, B. H., Marguerat, S., Stepanova, E., Davis, C. P., Bähler, J., Park, P. J., and Winston, F. (2013) Spt6 regulates intragenic and antisense transcription, nucleosome positioning, and histone modifications genome-wide in fission yeast. *Mol. Cell. Biol.* **33,** 4779–4792
40. Kato, H., Okazaki, K., Iida, T., Nakayama, J., Murakami, Y., and Urano, T. (2013) Spt6 prevents transcription-coupled loss of posttranslationally modified histone H3. *Sci. Rep.* **3,** 2186
41. Lopez, A. D., Tar, K., Krügel, U., Dange, T., Ros, I. G., and Schmidt, M. (2011) Proteasomal degradation of Sfp1 contributes to the repression of ribosome biogenesis during starvation and is mediated by the proteasome activator Blm10. *Mol. Biol. Cell* **22,** 528–540

42. Heck, J. W., Cheung, S. K., and Hampton, R. Y. (2010) Cytoplasmic protein quality control degradation mediated by parallel actions of the E3 ubiquitin ligases Ubr1 and San1. *Proc. Natl. Acad. Sci. U.S.A.* **107,** 1106–1111
43. Eisele, F., and Wolf, D. H. (2008) Degradation of misfolded protein in the cytoplasm is mediated by the ubiquitin ligase Ubr1. *FEBS Lett.* **582,** 4143–4146
44. Lee, Y. J., Lee, C. Y., Grzechnik, A., Gonzales-Zubiate, F., Vashisht, A. A., Lee, A., Wohlschlegel, J., and Chanfreau, G. F. (2013) RNA polymerase I stability couples cellular growth to metal availability. *Mol. Cell* **51,** 105–115
45. Yashiroda, H., Oguchi, T., Yasuda, Y., Toh, E. A., and Kikuchi, Y. (1996) Bul1, a new protein that binds to the Rsp5 ubiquitin ligase in *Saccharomyces cerevisiae. Mol. Cell. Biol.* **16,** 3255–3263
46. O'Donnell, A. F. (2012) The running of the Buls: control of permease trafficking by α-arrestins Bul1 and Bul2. *Mol. Cell. Biol.* **32,** 4506–4509
47. Cohen, M., Stutz, F., Belgareh, N., Haguenauer-Tsapis, R., and Dargemont, C. (2003) Ubp3 requires a cofactor, Bre5, to specifically de-ubiquitinate the COPII protein, Sec23. *Nat. Cell Biol.* **5,** 661–667
48. Bilsland, E., Hult, M., Bell, S. D., Sunnerhagen, P., and Downs, J. A. (2007) The Bre5/Ubp3 ubiquitin protease complex from budding yeast contributes to the cellular response to DNA damage. *DNA Repair* **6,** 1471–1484
49. Nostramo, R., Varia, S. N., Zhang, B., Emerson, M. M., and Herman, P. K. (2016) The catalytic activity of the Ubp3 deubiquitinating protease is required for efficient stress granule assembly in *Saccharomyces cerevisiae. Mol. Cell. Biol.* **36,** 173–183
50. Ossareh-Nazari, B., Niño, C. A., Bengtson, M. H., Lee, J. W., Joazeiro, C. A., and Dargemont, C. (2014) Ubiquitylation by the Ltn1 E3 ligase protects 60S ribosomes from starvation-induced selective autophagy. *J. Cell Biol.* **204,** 909–917
51. Isasa, M., Rose, C. M., Elsasser, S., Navarrete-Perea, J., Paulo, J. A., Finley, D. J., and Gygi, S. P. (2015) Multiplexed, proteome-wide protein expression profiling: yeast deubiquitylating enzyme knockout strains. *J. Proteome Res.* **14,** 5306–5317
52. Poulsen, J. W., Madsen, C. T., Young, C., Kelstrup, C. D., Grell, H. C., Henriksen, P., Juhl-Jensen, L., and Nielsen, M. L. (2012) Comprehensive profiling of proteome changes upon sequential deletion of deubiquitylating enzymes. *J. Proteomics* **75,** 3886–3897
53. Zhao, H., and Eide, D. (1996) The yeast *ZRT1* gene encodes the zinc transporter protein of a high-affinity uptake system induced by zinc limitation. *Proc. Natl. Acad. Sci. U.S.A.* **93,** 2454–2458
54. Hanscho, M., Ruckerbauer, D. E., Chauhan, N., Hofbauer, H. F., Krahulec, S., Nidetzky, B., Kohlwein, S. D., Zanghellini, J., and Natter, K. (2012) Nutritional requirements of the BY series of *Saccharomyces cerevisiae* strains for optimum growth. *FEMS Yeast Res.* **12,** 796–808
55. Gietz, D., St Jean, A., Woods, R. A., and Schiestl, R. H. (1992) Improved method for high efficiency transformation of intact yeast cells. *Nucleic Acids Res.* **20,** 1425
56. Goldstein, A. L., and McCusker, J. H. (1999) Three new dominant drug resistance cassettes for gene disruption in *Saccharomyces cerevisiae*. *Yeast* **15,** 1541–1553
57. Breslow, D. K., Cameron, D. M., Collins, S. R., Schuldiner, M., Stewart-Ornstein, J., Newman, H. W., Braun, S., Madhani, H. D., Krogan, N. J., and Weissman, J. S. (2008) A comprehensive strategy enabling high-resolution functional analysis of the yeast genome. *Nat. Methods* **5,** 711–718
58. Gasch, A. P., Spellman, P. T., Kao, C. M., Carmel-Harel, O., Eisen, M. B., Storz, G., Botstein, D., and Brown, P. O. (2000) Genomic expression programs in the response of yeast cells to environmental changes. *Mol. Biol. Cell* **11,** 4241–4257
59. Storici, F., Lewis, L. K., and Resnick, M. A. (2001) *In vivo* site-directed mutagenesis using oligonucleotides. *Nat. Biotechnol.* **19,** 773–776
60. Kaganovich, D., Kopito, R., and Frydman, J. (2008) Misfolded proteins partition between two distinct quality control compartments. *Nature* **454,** 1088–1095
61. Winston, F. (2008) EMS and UV mutagenesis in yeast. *Curr. Protoc. Mol. Biol.* **Chapter 13,** Unit 13.3B
62. Finley, D., Ozkaynak, E., and Varshavsky, A. (1987) The yeast polyubiquitin gene is essential for resistance to high temperatures, starvation, and other stresses. *Cell* **48,** 1035–1046
63. Collart, M. A., and Oliviero, S. (2001) Preparation of yeast RNA. *Curr. Protoc. Mol. Biol.* **Chapter 13,** Unit 13.12
64. Engels, W. R. (1993) Contributing software to the internet: the Amplify program. *Trends Biochem. Sci.* **18,** 448–450
65. Wong, M. L., and Medrano, J. F. (2005) Real-time PCR for mRNA quantitation. *BioTechniques* **39,** 75–85
66. Olivarius, S., Plessy, C., and Carninci, P. (2009) High-throughput verification of transcriptional starting sites by Deep-RACE. *BioTechniques* **46,** 130–132
67. Bailey, T. L., Boden, M., Buske, F. A., Frith, M., Grant, C. E., Clementi, L., Ren, J., Li, W. W., and Noble, W. S. (2009) MEME SUITE: tools for motif discovery and searching. *Nucleic Acids Res.* **37,** W202–W208